Article

# Design, Synthesis, and Antifungal Activity of 2,6-Dimethyl-4-aminopyrimidine Hydrazones as PDHc-E1 Inhibitors with a Novel Binding Mode

Yuan Zhou,[†] Shasha Zhang,[†] Meng Cai, Kaixing Wang, Jiangtao Feng, Dan Xie, Lingling Feng, Hao Peng, and Hongwu He*

Read Online

| ACCESS | | Metrics & More | | Article Recommendations | | SI Supporting Information |

**ABSTRACT:** A series of novel 2,6-dimethyl-4-aminopyrimidine hydrazones **5** were rationally designed and synthesized as pyruvate dehydrogenase complex E1 (PDHc-E1) inhibitors. Compounds **5** strongly inhibited *Escherichia coli* (*E. coli*) PDHc-E1 (IC$_{50}$ values 0.94−15.80 $\mu$M). As revealed by molecular docking, site-directed mutagenesis, enzymatic, and inhibition kinetic analyses, compounds **5** competitively inhibited PDHc-E1 and bound in a "straight" pattern at the *E. coli* PDHc-E1 active site, which is a new binding mode. In *in vitro* antifungal assays, most compounds **5** at 50 $\mu$g/mL showed more than 80% inhibition against the mycelial growth of six tested phytopathogenic fungi, including *Botrytis cinerea*, *Monilia fructigena*, *Colletotrichum gloeosporioides*, and *Botryosphaeria dothidea*. Notably, **5f** and **5i** were 1.8−380 fold more potent against *M. fructigena* than the commercial fungicides captan and chlorothalonil. In *vivo*, **5f** and **5i** controlled the growth of *M. fructigena* comparably to the commercial fungicide tebuconazole. Thus, **5f** and **5i** have potential commercial value for the control of peach brown rot caused by *M. fructigena*.

**KEYWORDS:** *2,6-dimethyl-4-aminopyrimidine hydrazones, PDHc-E1 inhibitor, antifungal activity, selectivity, molecular docking*

## 1. INTRODUCTION

Phytopathogenic fungi are of global concern as one of the most destructive plant-parasitic organisms and can cause persistent crop diseases and irreversible yield losses.[1,2] Although fungus-resistant crop varieties have been developed and other biological methods have been adopted to address these problems, chemical control remains one of the most effective methods to manage plant diseases.[3,4] However, the frequent use and the misuse of chemical fungicides have accelerated the emergence and development of resistant fungi, creating a considerable problem for the agricultural industry.[5,6] Therefore, it is desirable to develop fungicides with novel mechanisms of action to meet the needs of agricultural production.

The pyruvate dehydrogenase complex (PDHc) catalyzes the conversion of pyruvate into acetyl coenzyme A and is a key component of the energy metabolic pathway of organisms.[7] Pyruvate dehydrogenase E1 (PDHc-E1) is the first enzyme in the PDHc complex and catalyzes the only irreversible reaction of the complex, in conjunction with its cofactors thiamine diphosphate (ThDP) and Mg$^{2+}$.[8] Thus, PDHc-E1 in microorganisms is an important target in the design of fungicides. Captan is currently the only fungicide that targets the PDHc catalytic pathway,[9] but it is unknown whether it inhibits PDHc-E1 specifically. Because PDHc-E1 is an essential enzyme in energy metabolism, it is of interest to design and synthesize PDHc-E1 inhibitors to develop new fungicides. The reaction catalyzed by PDHc-E1 requires the cofactor ThDP,[10] and so the design and synthesis of ThDP analogues as competitive inhibitors may be a good strategy for the

development of novel fungicides targeting PDHc-E1. Most of the reported microbial PDHc-E1 inhibitors are ThDP analogues. However, the previously reported ThDP analogues (Figure 1, **IA−VIIG**) are difficult to synthesize because of their complex structures, and they show poor selectivity between microorganisms and mammals. These ThDP analogues also have low cellular uptake and bioavailability due to the presence of charged pyrophosphate moieties.[11−21] Therefore, to date, none of these compounds has been found to have fungicidal activity. The crystal structure of fungal PDHc-E1 has not been reported, but that of *Escherichia coli* PDHc-E1 (PDB: 1L8A) has been described.[22] Therefore, *E. coli* PDHc-E1 was chosen as the target microbial PDHc-E1 for the discovery of fungicides in our previous work. In those studies, several different series of ThDP analogues (Figure 1, **A1−I2**) were designed and synthesized as inhibitors of *E. coli* PDHc-E1.[23−34] Some of these compounds were found to have microbicidal activity. Compound **C** showed bactericidal activity, and compound **A2** was found to have higher *in vitro* inhibitory activity than that of pyrimethanil against the phytopathogenic fungus *Botrytis cinerea*.[24,26] However, the activities of these inhibitors were insufficient for commercial application as fungicides. There-
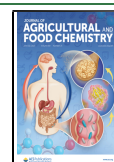
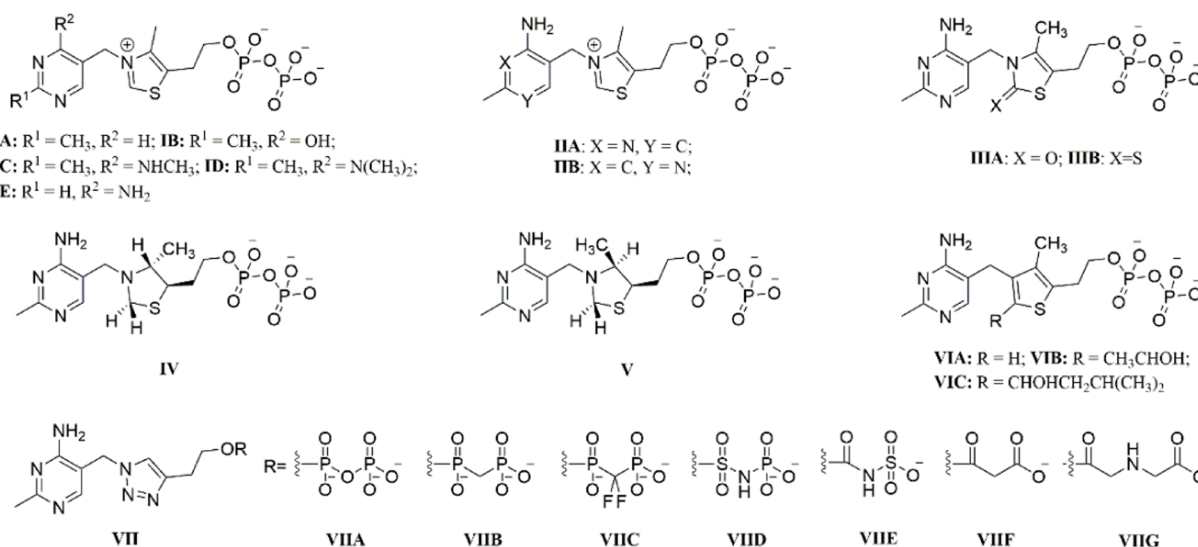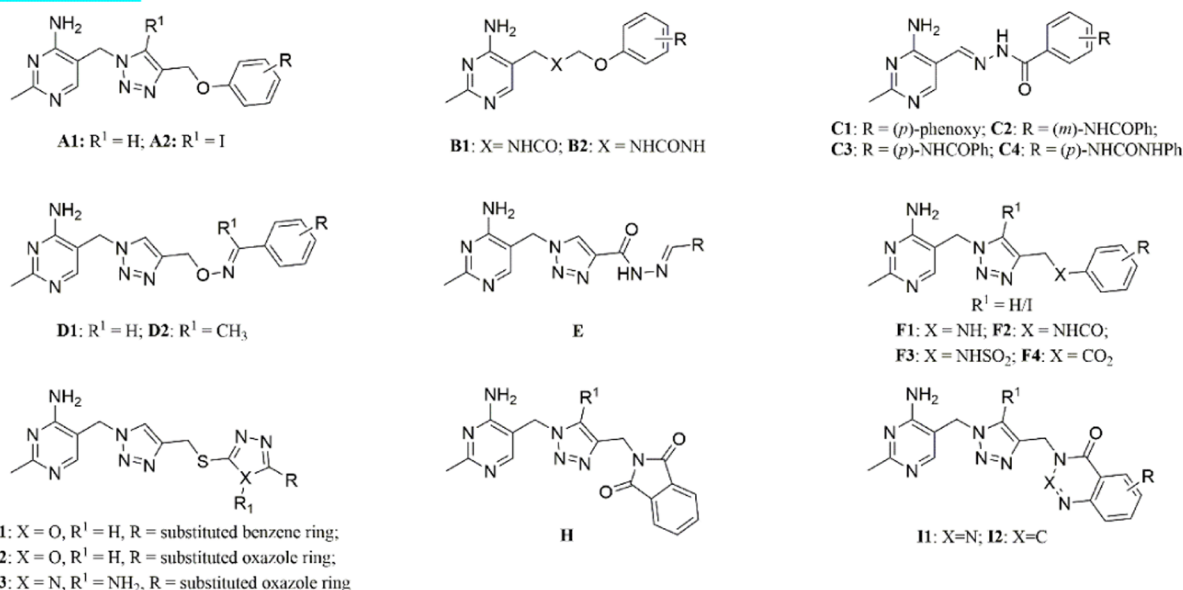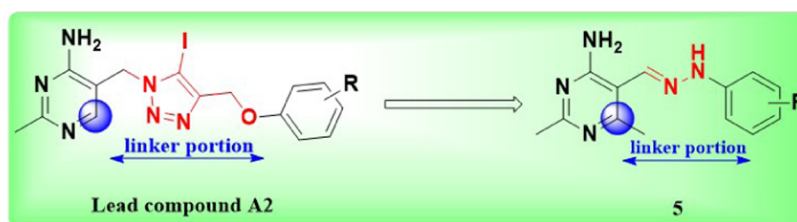**Figure 1.** Structure of ThDP analogues as PDHc-E1 inhibitors.



**Figure 2.** Design of the new 2,6-dimethyl-4-aminopyrimidine hydrazones **5**.

fore, **A2** was selected as the lead compound for optimization to improve its fungicidal activity.

The binding of these microbial PDHc-E1 inhibitors in the *E. coli* PDHc-E1 active site was systematically analyzed by molecular docking and crystal structure analyses. The results indicated that these analogues are similar to ThDP, binding in a "V" conformation in the *E. coli* PDHc-E1 active site with

multiple flexible bonds that easily rotate in the cavity.[22,24,25,28−37] Previous studies found that the aminopyrimidine ring in some PDHc-E1 inhibitors could form hydrogen bond interactions with the amino acid residues V192, M194, and E571 and a $\pi-\pi$ interaction with F602 in the active site of *E. coli* PDHc-E1.[27,28] Therefore, the aminopyrimidine ring was identified as an important active group for

PDHc-E1 inhibitors. To obtain PDHc-E1 inhibitors with higher fungicidal activity, we aimed to increase the inhibitory activity by optimizing the lead structure to enhance its interaction with the target enzyme.

Hydrazone derivatives with a conjugated structure (C=N−NH) usually show excellent fungicidal activity.[38,39] Therefore, we attempted to modify the lead compound **A2** by introducing a hydrazone moiety to replace the linker portion, thereby connecting the aminopyrimidine and benzene ring moieties directly (Figure 2). In view of the π−π interactions between aminopyrimidine ring and amino acid residues in the active site of PDHc-E1, it was speculated that these interactions may be further enhanced by introducing groups (e.g., CH₃, OH, NH₂, or OCH₃) into the aminopyrimidine ring.[40] We further introduced a methyl group at the 6-position of the aminopyrimidine ring to form a series of 2,6-dimethyl-4-aminopyrimidine hydrazones **5** (Figure 2). Within the **5** series, further optimization was focused on the modification of R.

We conducted a systematic analysis of title compounds in the **5** series, including their synthesis, inhibitory effects against *E. coli* PDHc-E1, selectivity for the target enzyme, and fungicidal activity. The interaction between compounds in the **5** series and *E. coli* PDHc-E1 was studied by molecular docking, site-directed mutagenesis, and enzyme inhibition kinetic analyses. Given that captan is currently the only fungicide that targets the PDHc catalytic pathway, compounds in the **5** series and captan were compared in terms of their targeting ability and fungicidal activity.

## 2. MATERIALS AND METHODS

**2.1. Chemistry.** All melting points (m.p.) were determined with a digital model X-5 apparatus (uncorrected). ¹H, ¹³C, and ¹⁹F nuclear magnetic resonance (NMR) spectra were recorded on a Bruker spectrometer at 400, 101, and 376 MHz with tetramethylsilane as the internal standard. Chemical shifts are reported in δ (parts per million (ppm)) values. A MicroMass GCT CA 055 instrument was used to acquire high-resolution electron impact mass spectra (HR-EIMS) under electron impact (70 eV) conditions. Crystal structures were obtained with a Bruker AEPEX DUO CCD diffractometer. All chemicals and reagents used for the syntheses were purchased from commercial sources, of analytical reagent (AR) grade, and used without further purification.

**2.2. Procedure for the Preparation of 2-(1-Ethoxyethylidene)malononitrile 1.** Compound **1** was prepared according to the reported procedure.[41] A mixture of malononitrile (10 g, 151.37 mmol) and triethyl orthoacetate (27.1 g, 167.05 mmol) was reacted at 90−95 °C for 45 min. Small-molecule impurities were then removed with a rotatory evaporator *in vacuo* at 60 °C to give 2-(1-ethoxyethylidene)malononitrile **1** as a pink solid (yield, 95%; m.p., 90−91 °C).

**2.3. General Procedure for Preparation of Substituted Phenylhydrazine Hydrochlorides 2.** Compounds **2** were prepared according to the reported procedure.[42] Concentrated HCl (50 mL) was added, under stirring, to a solution of the appropriately substituted aniline (20 mmol) at room temperature. The reaction mixture was cooled to 0 °C and treated with sodium nitrite solution (1.38 g, 20 mmol in 4 mL of water). The reaction mixture was stirred for 1 h to obtain a clear solution. Then, the cold diazonium salt solution was treated dropwise with a solution of stannous chloride dihydrate (10 g) in concentrated HCl (10 mL). The mixture was stirred for another 2 h. The corresponding phenylhydrazine hydrochloride **2** was collected by filtration and washed with saturated sodium chloride solution (15 mL). A series of **2** could be obtained by this procedure in yields of 40−65%.

**2.4. Procedure for the Preparation of 4-Amino-2,6-dimethylpyrimidine-5-carbonitrile 3.** Compound **3** was prepared according to the procedure previously reported.[26] To freshly prepared

sodium ethoxide solution (1.0 g, 0.0438 mol of sodium in 20 mL of absolute ethanol), acetamidine hydrochloride was added (3.87 g, 0.0409 mol). The reaction mixture was stirred at room temperature for 30 min, and the clear solution immediately turned turbid white. The solution was filtered and washed with 10 mL of absolute ethanol. The filtrate from the combined washings was used for further synthesis. To the filtrate, 2-(1-ethoxyethylidene)malononitrile **1** (5.57 g, 0.0409 mol) was added in portions over 15−20 min. A thick precipitate rapidly formed. After stirring for 3 h, the precipitate was collected by filtration, washed with small volumes of ethanol, and dried with suction under house vacuum to give 4-amino-2,6-dimethylpyrimidine-5-carbonitrile **3** (white solid; yield, 87%; m.p., 226−228 °C).

**2.5. Procedure for the Preparation of 4-Amino-2,6-dimethylpyrimidine-5-carbaldehyde 4.** Compound **4** was prepared according to the procedure previously reported.[26] Raney nickel (2.5 g of 50% slurry with water) was added to a solution of **3** (2.46 g, 0.0166 mol) in 85% formic acid (20 mL). The reaction mixture was refluxed until the disappearance of **3** was observed as monitored by thin-layer chromatography (TLC). The reaction mixture was filtered and washed with 10 mL of formic acid. The filtrate and washings were collected, combined, and concentrated under reduced pressure. The residue was purified by a silica gel column eluted with ethyl acetate/petroleum ether (1:1, v/v) to give 4-amino-2,6-dimethylpyrimidine-5-carbaldehyde **4** as a white solid (yield, 56%; m.p., 190−192 °C).

**2.6. General Procedure for the Synthesis of 2,6-Dimethyl-4-aminopyrimidine Hydrazones 5.** To a stirred suspension of appropriate substituted phenylhydrazine hydrochloride **2** (2 mmol) in ethanol (10 mL), triethylamine (Et₃N; 2 mmol, 0.20 g) was added. After 30 min of stirring at room temperature, 4-amino-2,6-dimethylpyrimidine-5-carbaldehyde **4** (2 mmol, 0.3 g) and six drops of acetic acid were added to the reaction mixture sequentially. The reaction mixture was refluxed until the disappearance of **4** was observed as monitored by TLC. The reaction mixture was poured into cold water (20 mL). The resulting precipitate was collected by filtration and dried under atmospheric pressure. The crude product was purified by recrystallization from ethanol to give the corresponding hydrazone **5**. The series of hydrazones **5** was obtained using this procedure.

*2.6.1. (E)-2,6-dimethyl-5-((2-phenylhydrazineylidene)methyl)-pyrimidin-4-amine (5a).* Yellow solid; yield 58%; m.p. 244−246 °C; ¹H NMR (400 MHz, dimethyl sulfoxide (DMSO)-$d_6$) δ (ppm): 2.31 (s, 3H, CH₃), 2.38 (s, 3H, CH₃), 6.74 (t, J = 7.3 Hz, 1H, Ar H), 6.88 (d, J = 7.6 Hz, 2H, Ar H), 7.21 (t, 2H, Ar H), 7.79 (s, 2H, NH₂), 8.24 (s, 1H, CH=N), 10.30 (s, 1H, NH); ¹³C NMR (100 MHz, DMSO-$d_6$) δ (ppm): 26.58, 30.58, 109.99, 116.57 (2C), 123.88, 134.29 (2C), 140.44, 149.71, 164.35, 167.21, 169.10; HRMS (ESI): calcd. for C₁₃H₁₅N₅ [M + H]⁺ 242.14002, found: 242.13980.

*2.6.2. (E)-5-((2-(3-fluorophenyl)hydrazineylidene)methyl)-2,6-dimethylpyrimidin-4-amine (5b).* Yellow solid; yield 62%; m.p. > 260 °C; ¹H NMR (400 MHz, DMSO-$d_6$) δ (ppm): 2.34 (s, 3H, CH₃), 2.40 (s, 3H, CH₃), 6.53−6.58 (m, 1H, Ar H), 6.67 (d, J = 11.5 Hz, 1H, Ar H), 6.73 (d, J = 8.2 Hz, 1H, Ar H), 7.26 (dd, J = 15.0, 8.0 Hz, 1H, Ar H), 7.79 (s, 2H, NH₂), 8.30 (s, 1H, CH=N), 10.54 (s, 1H, NH); ¹³C NMR (100 MHz, DMSO-$d_6$) δ (ppm): 21.74, 25.76, 98.51 (d, J = 26.0 Hz), 105.10, 105.38 (d, J = 21.4 Hz), 108.22 (d, J = 1.5 Hz), 131.40 (d, J = 10.2 Hz), 137.23, 147.16 (d, J = 11.0 Hz), 159.94, 162.65, 163.31, 165.05; ¹⁹F NMR (376 MHz, DMSO-$d_6$) δ (ppm): −112.25; HRMS (ESI): calcd. for C₁₃H₁₄FN₅ [M + H]⁺ 260.13060, found: 260.13056.

*2.6.3. (E)-5-((2-(4-fluorophenyl)hydrazineylidene)methyl)-2,6-dimethylpyrimidin-4-amine (5c).* Yellow solid; yield 78%; m.p. 217−219 °C; ¹H NMR (400 MHz, DMSO-$d_6$) δ (ppm): 2.55 (s, 3H, CH₃), 2.60 (s, 3H, CH₃), 6.97−7.01 (m, 2H, Ar H), 7.11 (t, J = 8.9 Hz, 2H, Ar H), 8.26 (s, 1H, CH=N), 9.25 (d, J = 138.5 Hz, 2H, NH₂), 11.15 (s, 1H, NH); ¹³C NMR (100 MHz, DMSO-$d_6$) δ (ppm): 16.45, 21.46, 106.52, 113.61 (d, J = 7.6 Hz, 2C), 116.37 (d, J = 22.6 Hz, 2C), 131.95, 141.12 (d, J = 1.4 Hz), 154.44 (d, J = 252.0 Hz), 158.03, 159.06, 160.59; ¹⁹F NMR (376 MHz, DMSO-$d_6$) δ

(ppm): −124.59; HRMS (ESI): calcd. for $C_{13}H_{14}FN_5$ [M + H]$^+$ 260.13060, found: 260.13011.

*2.6.4. (E)-5-((2-(2-chlorophenyl)hydrazineylidene)methyl)-2,6-dimethylpyrimidin-4-amine (5d).* Yellow solid; yield 61%; m.p. 255−257 °C; $^1$H NMR (400 MHz, DMSO-$d_6$) δ (ppm): 2.38 (s, 3H, CH$_3$), 2.45 (s, 3H, CH$_3$), 6.79−6.86 (m, 1H, Ar H), 7.22−7.31 (m, 2H, Ar H), 7.37 (dd, J = 7.9, 1.1 Hz, 1H, Ar H), 8.08 (s, 2H, NH$_2$), 8.79 (s, 1H, CH=N), 9.96 (s, 1H, NH); $^{13}$C NMR (100 MHz, DMSO-$d_6$) δ (ppm): 20.92, 25.06, 105.30, 113.39, 116.78, 120.31, 128.72, 130.07, 139.65, 141.19, 160.20, 162.34, 164.30; HRMS (ESI): calcd. for $C_{13}H_{14}ClN_5$ [M + H]$^+$ 276.10117.

*2.6.5. (E)-5-((2-(3-chlorophenyl)hydrazineylidene)methyl)-2,6-dimethylpyrimidin-4-amine (5e).* Yellow solid; yield 58%; m.p. 231−233 °C; $^1$H NMR (400 MHz, DMSO-$d_6$) δ (ppm): 2.36 (s, 3H, CH$_3$), 2.42 (s, 3H, CH$_3$), 6.79 (dd, J = 7.8, 1.2 Hz, 1H, Ar H), 6.86 (dd, J = 8.3, 1.2 Hz, 1H, Ar H), 6.91 (t, J = 1.9 Hz, 1H, Ar H), 7.25 (t, J = 8.0 Hz, 1H, Ar H), 7.97 (s, 2H, NH$_2$), 8.30 (s, 1H, CH=N), 10.65 (s, 1H, NH); $^{13}$C NMR (100 MHz, DMSO-$d_6$) δ (ppm): 21.13, 25.26, 105.22, 110.84, 111.27, 118.82, 131.42, 134.42, 136.97, 146.55, 160.05, 162.16, 164.36; HRMS (ESI): calcd. for $C_{13}H_{14}ClN_5$ [M + H]$^+$ 276.10105, found: 276.10067.

*2.6.6. (E)-5-((2-(4-chlorophenyl)hydrazineylidene)methyl)-2,6-dimethylpyrimidin-4-amine (5f).* Yellow solid; yield 86%; m.p. 235−236 °C; $^1$H NMR (400 MHz, DMSO-$d_6$) δ (ppm): 2.34 (s, 3H, CH$_3$), 2.40 (s, 3H, CH$_3$), 6.89 (d, J = 8.5 Hz, 2H, Ar H), 7.25 (d, J = 8.6 Hz, 2H, Ar H), 7.92 (s, 2H, NH$_2$), 8.23 (s, 1H, CH=N), 10.48 (s, 1H, NH); $^{13}$C NMR (100 MHz, DMSO-$d_6$) δ (ppm): 25.94, 30.04, 109.94, 118.04 (2C), 127.17, 134.09 (2C), 140.79, 148.50, 164.44, 166.26, 168.55; HRMS (ESI): calcd. for $C_{13}H_{14}ClN_5$ [M + H]$^+$ 276.10105, found: 276.10153.

*2.6.7. (E)-5-((2-(2-bromophenyl)hydrazineylidene)methyl)-2,6-dimethylpyrimidin-4-amine (5g).* Yellow solid; yield 63%; m.p. 231−233 °C; $^1$H NMR (400 MHz, DMSO-$d_6$) δ (ppm): 2.32 (s, 3H, CH$_3$), 2.40 (s, 3H, CH$_3$), 6.73 (td, J = 7.6, 1.5 Hz, 1H, Ar H), 7.17 (dd, J = 8.1, 1.3 Hz, 1H, Ar H), 7.29 (t, J = 7.7 Hz, 1H, Ar H), 7.49 (dd, J = 7.9, 1.3 Hz, 1H, Ar H), 7.78 (s, 2H, NH$_2$), 8.77 (s, 1H, CH=N), 9.63 (s, 1H, NH); $^{13}$C NMR (100 MHz, DMSO-$d_6$) δ (ppm): 26.71, 30.63, 109.73, 111.15, 118.27, 125.33, 133.76, 137.79, 144.97, 146.86, 164.53, 168.48, 169.72; HRMS (ESI): calcd. for $C_{13}H_{14}BrN_5$ [M + H]$^+$ 320.05053, found: 320.05048.

*2.6.8. (E)-5-((2-(3-bromophenyl)hydrazineylidene)methyl)-2,6-dimethylpyrimidin-4-amine (5h).* Yellow solid; yield 71%; m.p. 249−250 °C; $^1$H NMR (400 MHz, DMSO-$d_6$) δ (ppm): 2.40 (s, 3H, CH$_3$), 2.46 (s, 3H, CH$_3$), 6.94 (t, J = 8.4 Hz, 2H, Ar H), 7.07 (s, 1H, Ar H), 7.20 (t, J = 8.0 Hz, 1H, Ar H), 8.26 (s, 1H, CH=N), 8.36 (s, 2H, NH$_2$), 10.77 (s, 1H, NH); $^{13}$C NMR (100 MHz, DMSO-$d_6$) δ (ppm): 21.76, 25.76, 105.04, 111.08, 114.01, 121.54, 123.00, 131.68, 137.45, 146.70, 159.92, 163.34, 165.05; HRMS (ESI): calcd. for $C_{13}H_{14}BrN_5$ [M + H]$^+$ 320.05053, found: 320.04983.

*2.6.9. (E)-5-((2-(4-bromophenyl)hydrazineylidene)methyl)-2,6-dimethylpyrimidin-4-amine (5i).* Yellow solid; yield 78%; m.p. 244−246 °C; $^1$H NMR (400 MHz, DMSO-$d_6$) δ (ppm): 2.31 (s, 3H, CH$_3$), 2.38 (s, 3H, CH$_3$), 6.84 (d, J = 8.8 Hz, 2H, Ar H), 7.36 (d, J = 8.8 Hz, 2H, Ar H), 7.74 (s, 2H, NH$_2$), 8.24 (s, 1H, CH=N), 10.43 (s, 1H, NH); $^{13}$C NMR (100 MHz, DMSO-$d_6$) δ (ppm): 26.54, 30.52, 109.70, 114.55, 118.40 (2C), 136.85 (2C), 141.34, 148.86, 164.27, 167.49, 169.26; HRMS (ESI): calcd. for $C_{13}H_{14}BrN_5$ [M + H]$^+$ 320.05053, found: 320.05022.

*2.6.10. (E)-2,6-dimethyl-5-((2-(4-(trifluoromethyl)phenyl)-hydrazineylidene)methyl)pyrimidin -4-amine (5j).* Yellow solid; yield 82%; m.p. > 260 °C; $^1$H NMR (400 MHz, DMSO-$d_6$) δ (ppm): 2.32 (s, 3H, CH$_3$), 2.40 (s, 3H, CH$_3$), 7.01 (d, J = 8.5 Hz, 2H, Ar H), 7.54 (d, J = 8.6 Hz, 2H, Ar H), 7.78 (s, 2H, NH$_2$), 8.32 (s, 1H, CH=N), 10.74 (s, 1H, NH); $^{13}$C NMR (100 MHz, DMSO-$d_6$) δ (ppm): 21.75, 25.74, 104.94, 111.63 (2C), 118.91 (q, J = 32.1 Hz), 125.43 (q, J = 270.4 Hz), 127.12 (d, J = 3.7 Hz, 2C), 138.44, 148.04, 160.01, 163.67, 165.27; $^{19}$F NMR (376 MHz, DMSO-$d_6$) δ (ppm): −59.27; HRMS (ESI): calcd. for $C_{14}H_{14}F_3N_5$ [M + H]$^+$ 310.12741, found: 310.12701.

*2.6.11. (E)-2,6-dimethyl-5-((2-(4-nitrophenyl)hydrazineylidene)-methyl)pyrimidin-4-amine (5k).* Brown solid; yield 65%; m.p. >

260 °C; $^1$H NMR (400 MHz, DMSO-$d_6$) δ (ppm): 2.34 (s, 3H, CH$_3$), 2.42 (s, 3H, CH$_3$), 7.01 (d, J = 8.9 Hz, 2H, Ar H), 7.80 (s, 2H, NH$_2$), 8.14 (d, J = 9.1 Hz, 2H, Ar H), 8.43 (s, 1H, CH=N), 11.26 (s, 1H, NH); $^{13}$C NMR (100 MHz, DMSO-$d_6$) δ (ppm): 21.79, 25.80, 104.58, 111.27 (2C), 126.78 (2C), 138.76, 141.25, 150.22, 160.10, 164.55, 165.86; HRMS (ESI): calcd. for $C_{13}H_{14}N_6O_2$ [M + H]$^+$ 287.12510, found: 287.12477.

*2.6.12. (E)-2,6-dimethyl-5-((2-(o-tolyl)hydrazineylidene)methyl)-pyrimidin-4-amine (5l).* Yellow solid; yield 84%; m.p. 239−241 °C; $^1$H NMR (400 MHz, DMSO-$d_6$) δ (ppm): 2.25 (s, 3H, CH$_3$), 2.55 (s, 3H, CH$_3$), 2.60 (s, 3H, CH$_3$), 6.80 (t, J = 7.3 Hz, 1H, Ar H), 7.15 (dt, J = 12.3, 7.6 Hz, 3H, Ar H), 8.59 (s, 1H, CH=N), 9.39 (d, J = 117.6 Hz, 2H, NH$_2$), 10.08 (s, 1H, NH); $^{13}$C NMR (100 MHz, DMSO-$d_6$) δ (ppm): 16.49, 18.11, 21.47, 106.54, 111.70, 120.41, 121.97, 127.41, 131.14, 133.82, 142.32, 153.47, 159.14, 160.69; HRMS (ESI): calcd. for $C_{14}H_{17}N_5$ [M + H]$^+$ 256.15567, found: 256.15610.

*2.6.13. (E)-2,6-dimethyl-5-((2-(m-tolyl)hydrazineylidene)methyl)-pyrimidin-4-amine (5m).* Yellow solid; yield 75%; m.p. 178−180 °C; $^1$H NMR (400 MHz, DMSO-$d_6$) δ (ppm): 2.26 (s, 3H, CH$_3$), 2.32 (s, 3H, CH$_3$), 2.39 (s, 3H, CH$_3$), 6.59 (d, J = 7.4 Hz, 1H, Ar H), 6.71 (s, 2H, Ar H), 7.12 (t, J = 8.0 Hz, 1H, Ar H), 7.82 (s, 2H, NH$_2$), 8.26 (s, 1H, CH=N), 10.29 (s, 1H, NH); $^{13}$C NMR (100 MHz, DMSO-$d_6$) δ (ppm): 21.73, 21.85, 25.75, 105.42, 109.32, 112.52, 120.25, 129.65, 135.76, 138.93, 145.24, 159.90, 162.72, 164.64; HRMS (ESI): calcd. for $C_{14}H_{17}N_5$ [M + H]$^+$ 256.15567, found: 256.15577.

*2.6.14. (E)-2,6-dimethyl-5-((2-(p-tolyl)hydrazineylidene)methyl)-pyrimidin-4-amine (5n).* Yellow solid; yield 64%; m.p. 245−247 °C; $^1$H NMR (400 MHz, DMSO-$d_6$) δ (ppm): 2.21 (s, 3H, CH$_3$), 2.32 (s, 3H, CH$_3$), 2.38 (s, 3H, CH$_3$), 6.81 (d, J = 8.2 Hz, 2H, Ar H), 7.05 (d, J = 8.1 Hz, 2H, Ar H), 7.86 (s, 2H, NH$_2$), 8.23 (s, 1H, CH=N), 10.25 (s, 1H, NH); $^{13}$C NMR (100 MHz, DMSO-$d_6$) δ (ppm): 20.64, 21.68, 25.68, 105.41, 111.95 (2C), 127.87, 130.14 (2C), 135.19, 142.95, 159.80, 162.46, 164.44; HRMS (ESI): calcd. for $C_{14}H_{17}N_5$ [M + H]$^+$ 256.15567, found: 256.15540.

*2.6.15. (E)-5-((2-(4-methoxyphenyl)hydrazineylidene)methyl)-2,6-dimethylpyrimidin-4-amine (5o).* Yellow solid; yield 75%; m.p. 199−201 °C; $^1$H NMR (400 MHz, DMSO-$d_6$) δ (ppm): 2.54 (s, 3H, CH$_3$), 2.57 (s, 3H, CH$_3$), 3.70 (s, 3H, OCH$_3$), 6.92 (q, J = 9.0 Hz, 4H, Ar H), 8.12 (s, 1H, CH=N), 9.33 (d, J = 107.9 Hz, 2H, NH$_2$), 10.76 (s, 1H, NH); $^{13}$C NMR (100 MHz, DMSO-$d_6$) δ (ppm): 16.41, 21.38, 55.73, 106.72, 113.62 (2C), 115.29 (2C), 130.48, 138.30, 152.40, 153.82, 158.72, 160.58; HRMS (ESI): calcd. for $C_{14}H_{17}N_5O$ [M + H]$^+$ 272.15059, found: 272.15107.

*2.6.16. (E)-5-((2-(2,4-difluorophenyl)hydrazineylidene)methyl)-2,6-dimethylpyrimidin-4-amine (5p).* White solid; yield 54%; m.p. 232−233 °C; $^1$H NMR (400 MHz, DMSO-$d_6$) δ (ppm): 2.31 (s, 3H, CH$_3$), 2.36 (s, 3H, CH$_3$), 6.95−7.04 (m, 1H, Ar H), 7.10−7.26 (m, 2H, Ar H), 7.73 (s, 2H, NH$_2$), 8.54 (s, 1H, CH=N), 10.08 (s, 1H, NH); $^{13}$C NMR (100 MHz, DMSO-$d_6$) δ (ppm): 26.55, 30.58, 109.11 (t, J = 24.6 Hz), 109.70, 116.52 (d, J = 21.0 Hz), 118.16 (d, J = 4.7 Hz), 135.02 (d, J = 7.3 Hz), 143.70, 153.38 (dd, J = 241.8, 12.3 Hz), 159.56 (dd, J = 236.6, 11.1 Hz), 164.43, 167.93, 169.53; $^{19}$F NMR (376 MHz, DMSO-$d_6$) δ (ppm): −129.35, −123.70; HRMS (ESI): calcd. for $C_{13}H_{13}F_2N_5$ [M + H]$^+$ 278.12118, found: 278.12115.

*2.6.17. (E)-5-((2-(2,4-dichlorophenyl)hydrazineylidene)methyl)-2,6-dimethylpyrimidin-4-amine (5q).* White solid; yield 86%; m.p. 251−253 °C; $^1$H NMR (400 MHz, DMSO-$d_6$) δ (ppm): 2.33 (s, 3H, CH$_3$), 2.40 (s, 3H, CH$_3$), 7.22 (d, J = 8.8 Hz, 1H, Ar H), 7.34 (dd, J = 8.8, 2.3 Hz, 1H, Ar H), 7.50 (d, J = 2.3 Hz, 1H, Ar H), 7.76 (s, 2H, NH$_2$), 8.79 (s, 1H, CH=N), 9.98 (s, 1H, NH); $^{13}$C NMR (100 MHz, DMSO-$d_6$) δ (ppm): 21.85, 25.81, 104.93, 114.30, 117.15, 122.63, 128.73, 129.29, 140.50, 141.21, 160.10, 164.30, 165.51; HRMS (ESI): calcd. for $C_{13}H_{13}Cl_2N_5$ [M + H]$^+$ 310.06208, found: 310.06156.

**2.7. Crystallographic Study.** A colorless single crystal of **5i** suitable for X-ray analysis was crystallized from methanol at room temperature. Unit cell determination and data collection were performed using Mo Kα radiation (λ = 0.71073 Å) on a Bruker AEPEX DUO CCD diffractometer in π−ω scan mode at 296(2) K. The structure was solved directly using the SHELXS program of the
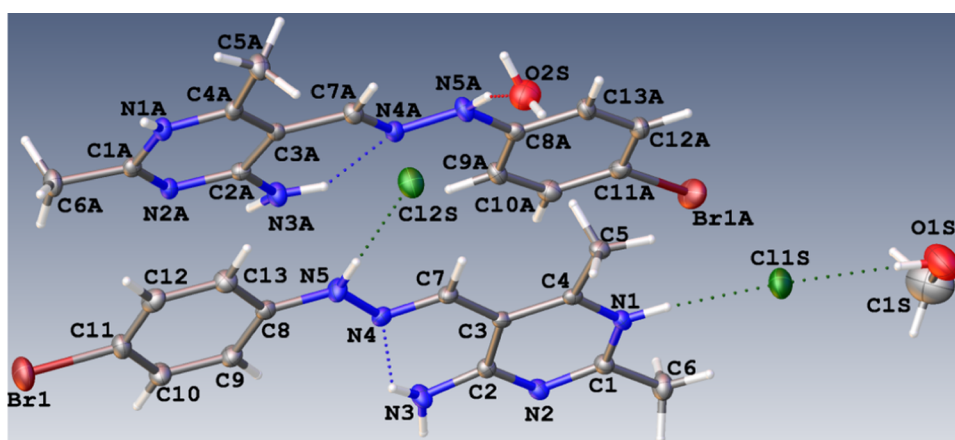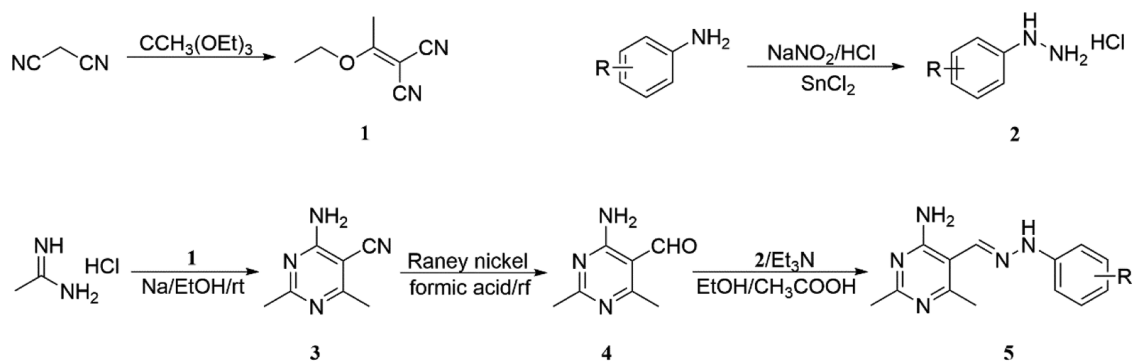
**Scheme 1. Synthesis of Title Compounds 5**





**Figure 3.** ORTEP molecular structure of **5i** shown as 30% thermal probability. The N—H···O, N—H···N, and N—H···Cl hydrogen bonds are shown as red, blue, and green dashed lines, respectively.

SHELXTL package and refined by full-matrix least-squares methods with SHELXL. The positions of all of the hydrogen atoms were determined from difference Fourier maps. All nonhydrogen atoms of **5i** were refined with anisotropic thermal parameters.

**2.8. Enzyme Inhibition Assay for PDHc-E1.** The half-maximal inhibitory concentration ($IC_{50}$) was determined in the presence of serial dilutions of the compounds (0–100 $\mu$M, 1‰ DMSO) and a reaction mix (50 mM $K_3PO_4$ (pH 6.4), 50 $\mu$M ThDP, 0.4 mM 2,6-dichlorophenolindophenol (DCIP), 50 $\mu$M sodium pyruvate substrate, and 5 $\mu$g of *E. coli* PDHc-E1) as described in a previous study.[43] *E. coli* PDHc-E1 was expressed from a pMal-C$_2$X-PDHc-E1 plasmid in *E. coli* TB1 cells and purified according to the method described by Ren et al.[43] The absorbance at 600 nm was measured using a BioTek reader (Synergy 2, BioTek Instruments Inc., VT), and the absorbance difference ($\Delta OD_{600}$) from the reduction of DCIP was calculated. $IC_{50}$ values were calculated by nonlinear curve fit of the data to the Hill kinetic equation using the Growth/Sigmoidal module of Origin 8.6 (OriginLab Corp., Northampton, MA) as described previously.[44]

The wild-type plasmid pMal-C$_2$X-PDHc-E1 constructed by Ren et al.[43] was used as a template for site-directed mutagenesis. The mutations V192A, M194A, E571A, Y599A, F602A, H640A, and E522A were introduced using a Fast Mutagenesis System (FM111-02, TransGen Biotech Co., Ltd., Beijing, China). The primers used for mutagenesis are listed in Table S2. The integrity and accuracy of the mutations were confirmed by DNA sequencing (Sangon Biotech (Shanghai) Co., Ltd., Shanghai, China). Mutant PDHc-E1 was expressed and purified in the same way as the wild-type PDHc-E1.
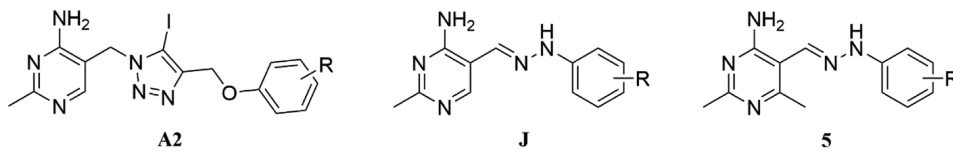
The inhibitory activity of compounds **5f**, **5h**, **5j**, **5k**, and **5p** against porcine PDHc-E1 was investigated according to the assay described by Zhou et al.[29] In general, the reaction mixture contained 1.0 mM MgCl$_2$, 50 mM K$_3$PO$_4$ (pH 7.0), 0.2 mM ThDP, 0.5 mM 3-(4,5-dimethylthiazol-2-yl)-2,5-diphenyltetrazolium bromide, 6.5 mM

phenazine methosulfate, 5 $\mu$L of porcine PDHc-E1 (P7032, Sigma-Aldrich (Shanghai) Co. LLC, Shanghai, China), and 100 $\mu$M test compound. After incubation at 37 °C for 3 min, 40 mM sodium pyruvate was added to start the reaction. The absorbance at 566 nm was measured using a BioTek reader (Synergy 2, BioTek Instruments Inc., VT). The inhibitory activity was calculated according to the method described in a previous study.[29]

**2.9. Determination of Inhibition Types.** Kinetic studies were carried out to determine the inhibition type of compound **5f** and ThDP. The kinetic assay runs were performed in the same manner as described in Section 2.8. The $\Delta OD_{600}$ values at various concentrations of ThDP (0, 0.1, 0.2, 0.4, 0.8, 2, 4, 10, 16, 22, 30, 50, and 100 $\mu$M) were evaluated for three different concentrations of **5f** (0, 1, and 2 $\mu$M). The maximum velocity ($V_{max}$) and Michaelis constant ($K_m$) values were calculated by fitting the data to the Hill kinetic equation using Origin 8.6 software.[32]

**2.10. Molecular Docking.** For the docking simulations, the chemical structures of the inhibitors were prepared by SYBYL 7.0 followed by 2000 steepest descent minimizations and 2000 conjugate gradient minimizations. The three-dimensional (3D) structure of *E. coli* PDHc-E1 was downloaded from the Protein Data Bank (PDB ID: 1L8A).[22] Homology modeling was performed to build the 3D structure of porcine PDHc-E1 using SWISS-MODEL.[45] Both the target structures were manipulated with Discovery Studio 4.0 to add missing hydrogens. Then, GLOD 3.0 was used to dock the constructed inhibitors into the active site. The radius of the active site was set to 10 Å using a genetic algorithm with 100 runs. The top-ranked conformation was selected as a representative.

**2.11. *In Vitro* Antifungal Assay.** The antifungal activity of the compounds against *Rhizoctonia solani*, *Botryosphaeria dothidea*, *B. cinerea*, *Magnaporthe poae*, *Colletotrichum gloeosporioides*, and *Monilia fructigena* was determined using mycelial growth assays. Mycelia plugs (5 mm in diameter) from the margin of pure colonies of each tested

**Table 1. Structures and Inhibitory Activities of A2, J, and 5 against *E. coli* PDHc-E1**



| compound | R | IC$_{50}$ ($\mu$M) |
|---|---|---|
| **A2-1** | H | 19.56 ± 0.00 |
| **A2-2** | 4-F | 7.85 ± 0.64 |
| **A2-3** | 2-Cl | 14.83 ± 0.91 |
| **A2-4** | 4-Cl | 11.86 ± 1.01 |
| **A2-5** | 2-Br | 15.69 ± 0.85 |
| **A2-6** | 4-Br | 4.21 ± 0.11 |
| **A2-7** | 4-NO$_2$ | 5.33 ± 0.00 |
| **A2-8** | 2,4-Cl$_2$ | 14.75 ± 0.03 |
| **J1** | H | 29.33 ± 0.12 |
| **J2** | 4-Cl | 32.65 ± 0.06 |
| **J3** | 3-Br | 22.56 ± 0.31 |
| **J4** | 4-Br | 26.45 ± 0.15 |
| **J5** | 4-NO$_2$ | 30.46 ± 0.17 |
| **J6** | 2,4-Cl$_2$ | >100 |
| **5a** | H | 5.70 ± 0.10 |
| **5b** | 3-F | 6.51 ± 0.77 |
| **5c** | 4-F | 5.62 ± 0.24 |
| **5d** | 2-Cl | 9.70 ± 0.63 |
| **5e** | 3-Cl | 3.24 ± 0.48 |
| **5f** | 4-Cl | 1.03 ± 0.15 |
| **5g** | 2-Br | 11.08 ± 0.34 |
| **5h** | 3-Br | 3.68 ± 0.11 |
| **5i** | 4-Br | 1.46 ± 0.23 |
| **5j** | 4-CF$_3$ | 0.94 ± 0.03 |
| **5k** | 4-NO$_2$ | 1.01 ± 0.06 |
| **5l** | 2-CH$_3$ | 11.21 ± 1.02 |
| **5m** | 3-CH$_3$ | 4.28 ± 0.44 |
| **5n** | 4-CH$_3$ | 3.36 ± 0.08 |
| **5o** | 4-OCH$_3$ | 15.80 ± 0.84 |
| **5p** | 2,4-F$_2$ | 3.07 ± 0.09 |
| **5q** | 2,4-Cl$_2$ | 6.69 ± 1.13 |
| **captan** | inhibition = 3.04% (100 $\mu$M) | |

fungus were excised and placed upside down in the center of fresh potato dextrose agar (PDA) plates, and solutions of the compounds **5** in DMSO were added at a series of concentrations. DMSO was used as a blank control. Each treatment was conducted in three replicate plates. The inhibitory activity of each compound against the mycelial growth was evaluated by measuring the colony diameters after 2–5 days of incubation in the dark at 25 or 20 °C. The inhibition rate was calculated according to the method described by He et al.[23] The effective concentration for 50% inhibition (EC$_{50}$) was calculated according to the method described by Cai et al.[46] Captan and another broad-spectrum fungicide chlorothalonil were used as positive controls.

**2.12. *In Vivo* Antifungal Assay.** Healthy, mature, and firm peach fruits called "Jinqiuhong peaches" were purchased from Qingdao, Shandong Province. The fruits were first washed twice with distilled water and then surface-disinfected with 75% ethanol (v/v) for 30 s and 1% sodium hypochlorite (v/v) for 30 s, followed by rinsing three times with sterile distilled water and natural drying. Two wounds (8 mm in diameter by 5 mm deep) were inflicted at opposite sides of each fruit using a sterile cork borer, and the fruits were inoculated with a mycelium plug of the same size excised from the margin of a 6 day old culture. Compounds **5i** and **5f** (10, 5, and 2.5 $\mu$g/mL) were sprayed onto the fruits, 1 h prior to inoculation. The commercial fungicide tebuconazole (10, 5, and 2.5 $\mu$g/mL) was used as a

comparison. DMSO was used as a blank control. After inoculation, the fruits were placed into plastic boxes with wet sterile cotton to maintain high humidity and were incubated in a 20 °C chamber. The lesion diameters were measured after 96 h, and the control efficiency was calculated. Each test was performed in quadruplicate.[47]

## 3. RESULTS AND DISCUSSION

**3.1. Chemistry. *3.1.1. Synthesis.*** Seventeen compounds of **5** as ThDP analogues were designed and synthesized by a simple and convenient synthetic route (Scheme 1).

4-Amino-2,6-dimethylpyrimidine-5-carbaldehyde **4** is the key intermediate for the synthesis of **5**. Condensation of malononitrile and triethyl orthoacetate yielded 2-(1-ethoxyethylidene)malononitrile **1**, which was then reacted with acetamidine hydrochloride in ethanol to give 4-amino-2,6-dimethylpyrimidine-5-carbonitrile **3**. Then, **3** was converted to **4** using Raney nickel with 80–85% formic acid as the solvent. The synthesis of the substituted phenylhydrazine hydrochlorides **2** was carried out by the reduction of the diazonium salt of the respective substituted aniline with stannous chloride. Finally, compounds **5** were synthesized by reacting **4** with the respective substituted phenylhydrazine hydrochlorides **2** via
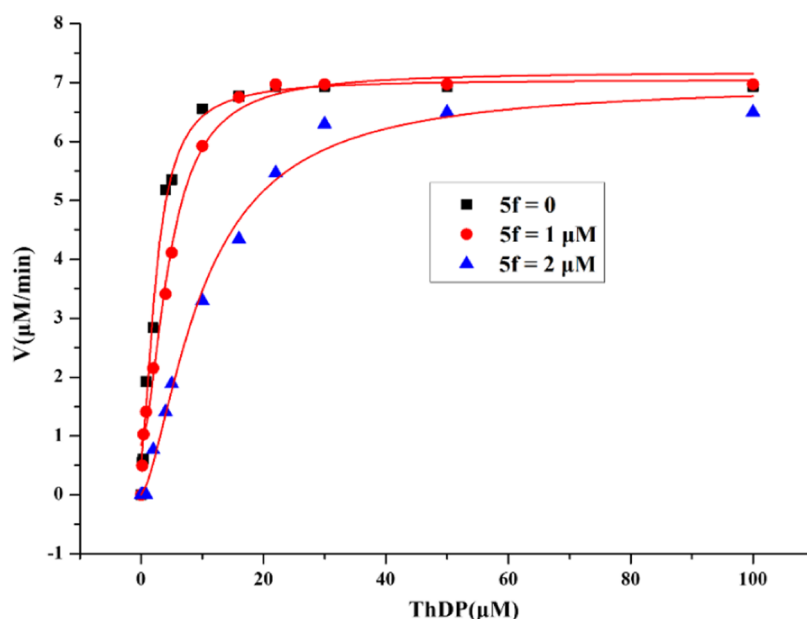
**Figure 4.** Enzyme kinetics experimental data of **5f** against *E. coli* PDHc-E1.

**Table 2. $V_{max}$ and $K_m$ Values of Compound 5f against *E. coli* PDHc-E1**

| compound | concentration ($\mu$M) | $V_{max}$ ($\mu$M/min/mg) | $K_m$ ($\mu$M) |
|---|---|---|---|
| **5f** | 0 | 7.50 ± 0.30 | 2.38 ± 0.31 |
| | 1 | 8.87 ± 0.87 | 5.66 ± 1.52 |
| | 2 | 7.70 ± 0.52 | 11.99 ± 1.61 |

**Table 3. Inhibition of 5 against *E. coli* and Porcine PDHc-E1**

| | *E. coli* PDHc-E1 | | porcine PDHc-E1 |
|---|---|---|---|
| compound | $IC_{50}$ ($\mu$M) | inhibitory potency[a] (%) | inhibitory potency[a] (%) |
| **5f** | 1.03 ± 0.15 | 100.00 ± 0.45 | 14.89 ± 7.74 |
| **5h** | 3.68 ± 0.11 | 100.00 ± 0.62 | 13.60 ± 7.32 |
| **5j** | 0.94 ± 0.03 | 100.00 ± 0.95 | 20.05 ± 2.95 |
| **5k** | 1.01 ± 0.06 | 100.00 ± 0.03 | 10.38 ± 4.03 |
| **5p** | 3.07 ± 0.09 | 100.00 ± 0.98 | 25.21 ± 5.91 |

[a]Inhibitory potency (%) of compounds against enzyme *in vitro* at 100 $\mu$M as an average of triplicate.

nucleophilic addition in the presence of Et₃N and acetic acid. In this nucleophilic addition, a hemiaminal was first formed, followed by dehydration to give the −C=N−NH− bond.

*3.1.2. Crystal Structure of Compound 5i.* Crystal data for **5i** are presented in Table S1, while Figure 3 provides a perspective view based on the atomic labeling system (CCDC-1907627; these data are available free of charge from the Cambridge Crystallographic Data Centre). As shown in the crystal structure of **5i**, the entire molecule lies in the same plane in a linear structure, presenting a considerable difference from the configurations of previously reported ThDP-derived PDHc-E1 inhibitors (which have V-shaped crystal structures).[29,34]

Single-crystal diffraction analysis indicated that compound **5i** is crystallized in the monoclinic $P2_1/c$ space group. Its asymmetric crystal structure unit consists of two 2,6-dimethyl-4-aminopyrimidine hydrazone cations with the protonated N1 at the 3-position of the aminopyrimidine rings, as well as two chloride anions, one methanol, and one water solvent molecule. The bond lengths around N1 and N2 atoms ($d_{N1-C4} = 1.354(6)$ Å, $d_{N1-C1} = 1.334(6)$ Å, and $d_{N2-C2} = 1.352(6)$ Å, $d_{N2-C1} = 1.296(6)$ Å) indicate the 3-position protonation of atom N1. The torsional angles of $\varphi_{N5-N4-C7-C3} = 178.6(4)°$ and $\varphi_{C7-N4-N5-C8} = -178.6(5)°$ indicate that the two lateral aromatic rings are in the "E" configuration with a dihedral angle of only 3.6(1)° between them. A Cambridge Structural Database (CSD) analysis of aromatic hydrazones
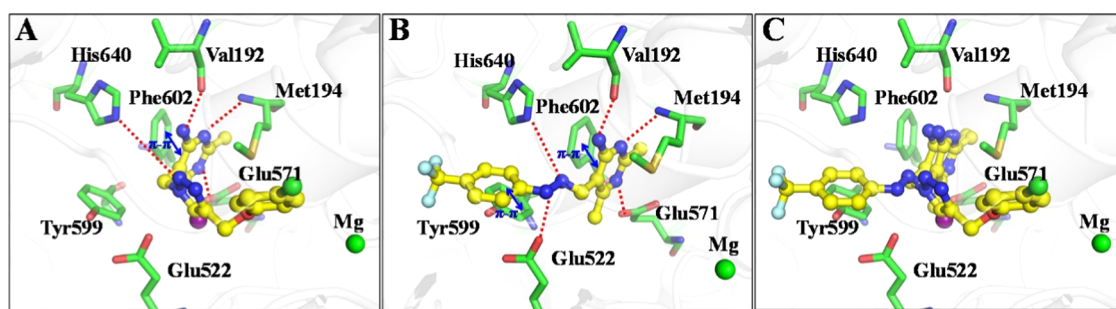


**Figure 5.** Optimal binding model for compounds **A2-4** (A) and **5j** (B) in the active site of *E. coli* PDHc-E1 docked by GOLD 3.0. The binding model for compounds **A2-4** and **5j** (C) simultaneously at the active site of *E. coli* PDHc-E1. PDHc-E1 is shown as a ribbon, the ligands and some key residues are shown in stick form, and hydrogen bonds are shown as dashed lines.
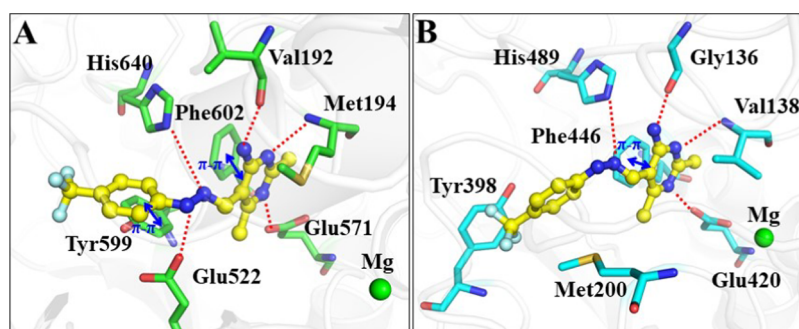
**Figure 6.** Optimal binding models for compound **5j** at the active site of *E. coli* PDHc-E1 (A) and porcine PDHc-E1 (B) docked by GOLD 3.0. PDHc-E1 is shown as ribbon, ligands and some key residues are shown as sticks, and hydrogen bonds are shown as dashed lines.
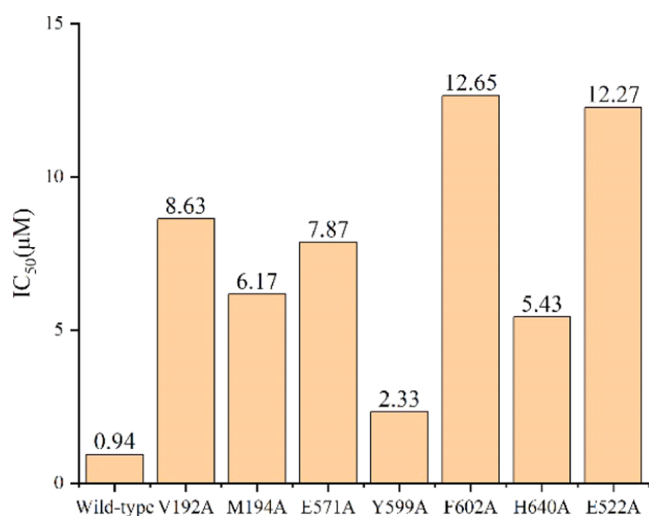


**Figure 7.** IC$_{50}$ values of **5j** against wild-type *E. coli* PDHc-E1 and its mutants. The substrate is pyruvate acid, and the cofactor is ThDP.

showed that there are more than 300 analogues with good planar structures. From the results, we concluded that the planarity may be largely attributed to the central hydrazone-related conjugated double bond.

In the crystal packing of **5i**, the component ions are linked into a complex three-dimensional hydrogen-bonded network by a combination of N−H···O/N/Cl and O−H···Cl hydrogen bonds. Additionally, the network is further consolidated by several π···π interactions. For instance, two centrally related pyrimidine (N1/N2/C1−C4) rings are closely stacked with a centroid-to-centroid distance of only 3.504(3) Å and a slippage distance of 0.984(1) Å, indicating a strong intermolecular noncovalent interaction between them. Additionally, the $^1$H NMR signal spectrum was consistent with the free compound **5i** molecule, indicating that the protonated molecule is redeprotonated in solution.

**3.2. Inhibitory Activity against *E. coli* PDHc-E1.** The inhibitory activity of compounds **5a−q** against *E. coli* PDHc-E1 was evaluated. The IC$_{50}$ values are summarized in Table 1. The compounds showed excellent inhibitory activities (IC$_{50}$ = 0.94−15.80 μM) against *E. coli* PDHc-E1. Compound **5j** (R = 4-CF$_3$) exhibited the strongest inhibitory activity with an IC$_{50}$ of 0.94 μM.

Compared with the lead compound **A2**,[24] the compounds in series **5** exhibited stronger inhibitory activity against *E. coli* PDHc-E1 when the R substituents were the same, e.g., **5a** (R = H, IC$_{50}$ = 5.70 ± 0.10 μM) > **A2-1** (R = H, IC$_{50}$ = 19.56 ±

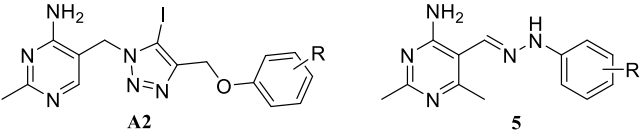**Table 4. Preliminary Antifungal Activities of Compounds 5 at 50 μg/mL**
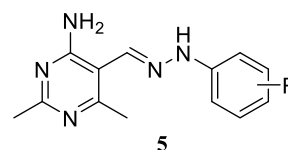


| compound | R | average values of inhibition rate (%) to six pathogens[a] | | | | | |
|---|---|---|---|---|---|---|---|
| | | R. s.[b] | B. d.[b] | B. c.[b] | M. p.[b] | C. g.[b] | M. f.[b] |
| **5a** | H | 68.4 | 73.8 | 63.3 | 36.6 | 95.4 | 74.8 |
| **5b** | 3-F | 76.8 | 66.6 | 84.3 | 48.3 | 73.0 | 85.6 |
| **5c** | 4-F | 79.1 | 83.2 | 66.2 | 79.6 | 82.8 | 14.6 |
| **5d** | 2-Cl | 79.3 | 58.9 | 76.6 | 79.0 | 35.1 | 20.8 |
| **5e** | 3-Cl | 67.0 | 65.2 | 78.9 | 76.0 | 47.2 | 90.2 |
| **5f** | 4-Cl | 58.6 | 74.1 | 85.7 | 33.6 | 54.6 | 86.9 |
| **5g** | 2-Br | 44.9 | 46.8 | 75.5 | 47.8 | 82.7 | 85.9 |
| **5h** | 3-Br | 7.13 | 0 | 0 | 0 | 32.7 | 85.9 |
| **5i** | 4-Br | 52.2 | 69.5 | 64.3 | 28.4 | 59.2 | 85.9 |
| **5j** | 4-CF$_3$ | 75.6 | 80.5 | 83.7 | 66.4 | 48.5 | 88.9 |
| **5k** | 4-NO$_2$ | 32.1 | 72.1 | 47.6 | 12.8 | 76.5 | 80.3 |
| **5l** | 2-CH$_3$ | 55.0 | 0 | 74.9 | 55.9 | 35.9 | 88.9 |
| **5m** | 3-CH$_3$ | 56.0 | 0 | 75.2 | 55.0 | 35.2 | 88.9 |
| **5n** | 4-CH$_3$ | 67.6 | 76.1 | 80.7 | 64.0 | 81.9 | 30.8 |
| **5o** | 4-OCH$_3$ | 45.9 | 23.2 | 83.0 | 45.0 | 88.9 | 87.0 |
| **5p** | 2,4-F$_2$ | 70.3 | 55.0 | 83.2 | 63.4 | 77.6 | 90.9 |
| **5q** | 2,4-Cl$_2$ | 48.6 | 36.9 | 53.1 | 0 | 32.7 | 88.9 |

[a]Inhibitory potency (%) against the growth of pathogenic fungi, 0 (no effect), 100% (completely kill). [b]R. s., *Rhizoctonia solani*; B. d., *Botryosphaeria dothidea*; B. c., *Botrytis cinerea*; M. p., *Magnaporthe poae*; C. g., *Colletotrichum gloeosporioides*; M. f., *Monilia fructigena*.
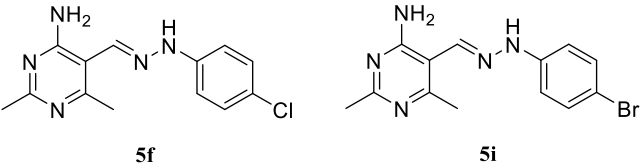
0.00 μM), **5c** (R = 4-F, IC$_{50}$ = 5.62 ± 0.24 μM) > **A2-2** (R = 4-F, IC$_{50}$ = 7.85 ± 0.64 μM), and **5d** (R = 2-Cl, IC$_{50}$ = 9.70 ± 0.63 μM) > **A2-3** (R = 2-Cl, IC$_{50}$ = 14.83 ± 0.91 μM). The inhibitory activity against *E. coli* PDHc-E1 was increased by optimizing the linker portion and aminopyrimidine ring in the **A2** parent structure, in line with our hypothesis. Captan inhibited *E. coli* PDHc-E1 by only 3.04% at a concentration of 100 μM, indicating that captan does not target PDHc-E1 specifically.

The analysis of structure−activity relationships for the compounds in series **5** indicated that inhibitory activity against *E. coli* PDHc-E1 was highly dependent upon the structure and position of the R substituent on the benzene ring. Compounds with the same R substituent at the 4-position of the benzene ring displayed stronger inhibitory activity against *E. coli* PDHc-

**Table 5. EC$_{50}$ Values of 2,6-Dimethyl-4-aminopyrimidine Hydrazones and A2-4 against Five Plant Phytopathogenic Fungi**



| compound | R | EC$_{50}$ ($\mu$M) | | | | |
| --- | --- | --- | --- | --- | --- | --- |
| | | B. d.[a] | B. c.[a] | M. p.[a] | C. g.[a] | M. f.[a] |
| A2-4 | 4-Cl | >100 | 11.80 | >100 | >100 | >100 |
| 5a | H | >30 | >30 | >50 | 53.60 | >30 |
| 5b | 3-F | >30 | 24.35 | >50 | >25 | 5.65 |
| 5c | 4-F | 3.72 | >30 | >20 | 32.80 | >100 |
| 5e | 3-Cl | >30 | >20 | >20 | >50 | 7.55 |
| 5f | 4-Cl | 12.24 | 6.53 | 63.34 | >30 | 0.25 |
| 5g | 2-Br | >50 | >20 | >50 | >20 | 33 |
| 5h | 3-Br | NA[b] | NA[b] | NA[b] | >50 | 7.28 |
| 5i | 4-Br | >30 | >30 | >50 | >30 | 1.15 |
| 5j | 4-CF$_3$ | >20 | 4.33 | >30 | >50 | 5.39 |
| 5k | 4-NO$_2$ | >30 | >50 | NA | >30 | 36.68 |
| 5l | 2-CH$_3$ | NA[b] | >20 | >30 | >50 | 8.99 |
| 5m | 3-CH$_3$ | NA[b] | >20 | >30 | >50 | 12.44 |
| 5n | 4-CH$_3$ | >20 | 4.70 | >30 | 11.90 | >100 |
| 5o | 4-OCH$_3$ | NA | 8.30 | >50 | 16.97 | 45.97 |
| 5p | 2,4-F$_2$ | >30 | 15.10 | >30 | >20 | 5.55 |
| captan | | 70.50 | 117.60 | >150 | >150 | 95 |
| chlorothalonil | | 4.06 | 3.57 | 52.40 | 52.40 | 2.11 |

[a]B. d., *Botryosphaeria dothidea*; B. c., *Botrytis cinerea*; M. p., *Magnaporthe poae*; C. g., *Colletotrichum gloeosporioides*; M. f., *Monilia fructigena*. [b]NA: not active.

**Table 6. Control Efficiency of 5f and 5i against *M. fructigena* on Peach Fruits**



| treatment | rate ($\mu$g/mL) | control efficiency (%) (4 DAT)[a][b][c] | | | | | significant difference[d] |
| --- | --- | --- | --- | --- | --- | --- | --- |
| | | replicate 1 | replicate 2 | replicate 3 | replicate 4 | average | |
| tebuconazole | 2.5 | 86.93 | 85.62 | 86.93 | 52.94 | 78.10 | ab |
| | 5 | 90.85 | 81.7 | 83.01 | 83.01 | 84.64 | ab |
| | 10 | 93.46 | 93.46 | 96.08 | 97.39 | 95.10 | a |
| 5f | 2.5 | 94.77 | 96.08 | 81.7 | 90.85 | 90.85 | a |
| | 5 | 94.77 | 85.62 | 77.78 | 77.78 | 83.99 | ab |
| | 10 | 85.62 | 85.62 | 94.77 | 76.47 | 85.62 | ab |
| 5i | 2.5 | 63.4 | 90.85 | 45.1 | 89.54 | 72.22 | b |
| | 5 | 94.77 | 88.24 | 85.62 | 88.24 | 89.22 | ab |
| | 10 | 90.85 | 90.85 | 94.77 | 86.93 | 90.85 | a |

[a]The control efficiency (%) of compounds against *M. fructigena* was measured as the percentage change in the diameter of each peach lesion compared with that of the blank control (DMSO); values are the average of four replicates. [b]The peach fruits called Jinqiuhong peaches were purchased from Qingdao, Shandong Province. The tests were performed in the middle of November 2019 at Wu Han, Hubei. [c]DAT is day after treatment. [d]The column followed by the same letters indicates no significant differences between the average values according to Tukey's honestly significant difference test ($P = 0.05$).

E1 than did those with the R substituent at the 3-position. Similarly, those with the same R substituent at the 3-position of the benzene ring displayed stronger inhibitory activity against *E. coli* PDHc-E1 than did those with the R substituent at the 2-position, e.g., **5f** (R = 4-Cl, IC$_{50}$ = 1.03 ± 0.15 $\mu$M) > **5e** (R = 3-Cl, IC$_{50}$ = 3.24 ± 0.48 $\mu$M) > **5d** (R = 2-Cl, IC$_{50}$ = 9.70 ± 0.63 $\mu$M); **5i** (R = 4-Br, IC$_{50}$ = 1.46 ± 0.23 $\mu$M) > **5h** (R = 3-Br, IC$_{50}$ = 3.68 ± 0.11 $\mu$M) > **5g** (R = 2-Br, IC$_{50}$ =

11.08 ± 0.34 $\mu$M); and **5n** (R = 4-CH$_3$, IC$_{50}$ = 3.36 ± 0.08 $\mu$M) > **5m** (R = 3-CH$_3$, IC$_{50}$ = 4.28 ± 0.44 $\mu$M) > **5l** (R = 2-CH$_3$, IC$_{50}$ = 11.21 ± 1.02 $\mu$M). The different R substituents also greatly affected the inhibitory activity against *E. coli* PDHc-E1. For example, when different halogens (F, Cl, or Br) were present at the 4-position of the benzene ring, the inhibitory activity of compounds **5f** (R = 4-Cl, IC$_{50}$ = 1.03 ± 0.15 $\mu$M) and **5i** (R = 4-Br, IC$_{50}$ = 1.46 ± 0.23 $\mu$M) was higher
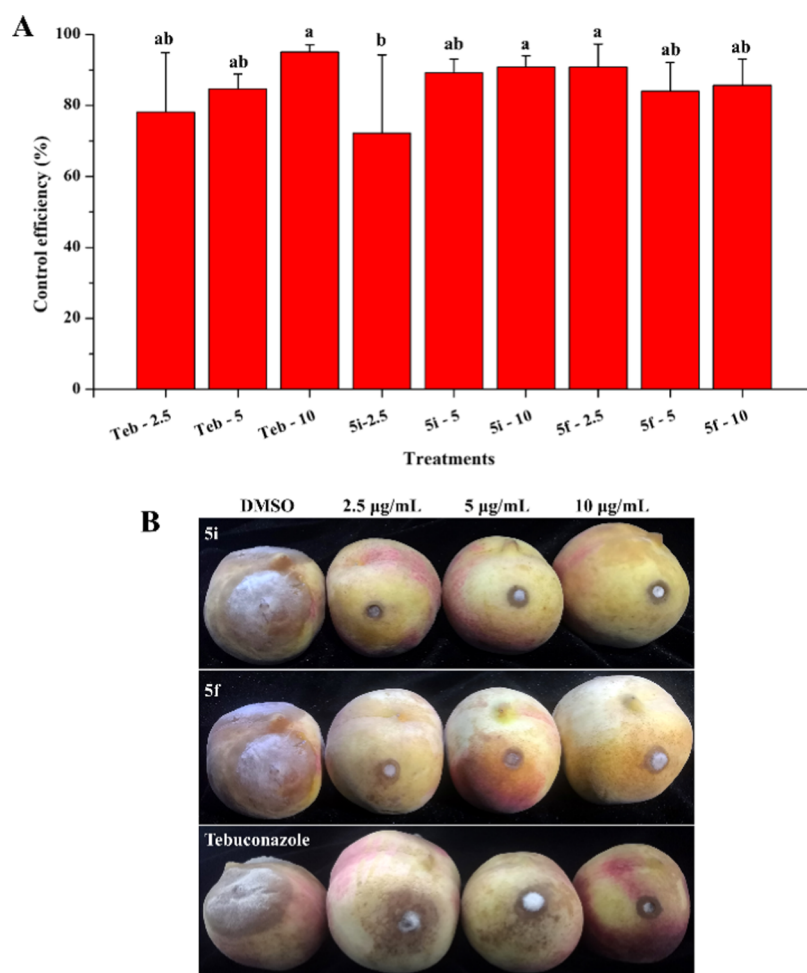
**Figure 8.** Control efficiency of **5i** and **5f** against *M. fructigena* on peach fruit after 4 days of treatment.

than that of **5c** (R = 4-F, $IC_{50}$ = 5.62 ± 0.24 $\mu$M). In most instances, an electron-withdrawing group as R in compounds in the **5** series enhanced inhibitory activity against *E. coli* PDHc-E1.

To further confirm the role of the methyl group at the 6-position of the 4-aminopyrimidine ring in title compound **5**, the inhibitory activities of 2-methyl-4-aminopyrimidine hydrazones **J** and **5** against *E. coli* PDHc-E1 were compared. As shown in Table 1, compounds **J1**−**J6** weakly inhibited *E. coli* PDHc-E1 with $IC_{50}$ values ranging from 22.56 to 100 $\mu$M.[48] Compared with **J1**−**J6**, the corresponding **5a**, **5f**, **5h**, **5i**, **5k**, and **5q** showed stronger inhibitory activities against *E. coli* PDHc-E1 when their R substituents were the same. This result confirmed that the newly introduced methyl group at the 6-position of 4-aminopyrimidine ring strengthened the inhibitory activity against *E. coli* PDHc-E1.

**3.3. Inhibitory Mechanism of Compounds.** To determine the inhibitory mechanism of compounds in the **5** series, **5f** was selected to study its kinetic inhibition against *E. coli* PDHc-E1. The values of the $V_{max}$ and $K_m$ in the presence and absence of **5f** were determined.

The Michaelis−Menten equation curves are shown in Figure 4, and the $V_{max}$ and $K_m$ values are listed in Table 2. As shown in Table 2, the $V_{max}$ values remained nearly constant in the presence or absence of **5f**, while the $K_m$ values increased as the concentration of **5f** increased. On the basis of these

observations, we concluded that **5f** acts as a competitive inhibitor of ThDP against *E. coli* PDHc-E1.

**3.4. Selectivity of Compounds.** Many of the previously reported ThDP analogues that function as PDHc-E1 inhibitors show poor selectivity between PDHc-E1 from microbes and mammals. For example, the ThDP analogue **IIIB** (Figure 1) showed strong inhibitory activity against both *E. coli* PDHc-E1 ($K_i$ = 64 nM) and human PDHc-E1 ($K_i$ = 74 nM).[15,22] To address this issue, several series of ThDP analogues as PDHc-E1 inhibitors, including compounds **A, C, F, G, H,** and **I** (Figure 1), were designed and synthesized in our previous work. All of these compounds showed weaker inhibitory activity against mammalian PDHc-E1 than against microbial PDHc-E1.[24,26,29,33,34] In this work, the selectivity of the compounds in the **5** series was examined.

Compounds **5f** ($IC_{50}$ = 1.03 ± 0.15 $\mu$M), **5h** ($IC_{50}$ = 3.68 ± 0.11 $\mu$M), **5j** ($IC_{50}$ = 0.94 ± 0.03 $\mu$M), **5k** ($IC_{50}$ = 1.01 ± 0.06 $\mu$M), and **5p** ($IC_{50}$ = 3.07 ± 0.09 $\mu$M) with excellent inhibitory activity against *E. coli* PDHc-E1 were selected to investigate their inhibitory activity against porcine PDHc-E1 (Table 3). At a concentration of 100 $\mu$M, all of these compounds exhibited 100% inhibition against *E. coli* PDHc-E1 but <30% inhibition against porcine PDHc-E1. This result showed that compounds in the **5** series can selectively inhibit *E. coli* PDHc-E1 and may have low toxicity toward mammals.

**3.5. Analysis of Interactions.** To clarify how the compounds in the **5** series interact with the target enzyme,

**5j** with the strongest inhibitory activity was selected for analysis of its docking into the active site of *E. coli* PDHc-E1. For comparison, the molecular docking of **A2-4** was also investigated. As shown in Figure 5, both compounds **A2-4** and **5j** were able to bind in the ThDP pocket. Compound **A2-4** bound in the *E. coli* PDHc-E1 active site in a V conformation similar to ThDP, and the 4-aminopyrimidine ring was able to form hydrogen bond interactions with the amino acid residues V192, M194, and E571 and a $\pi-\pi$ interaction with F602, similar to the interactions of ThDP (Figure 5A). The N atom of the 1,2,3-triazole ring in **A2-4** formed a weak hydrogen bond interaction with H640. By contrast, although the aminopyrimidine ring in **5j** could also form interactions with the amino acid residues V192, M194, E571, and F602, similar to **A2-4**, the entire molecule **5j** bound in a straight conformation in the *E. coli* PDHc-E1 active site, considerably different from the case for **A2-4** and ThDP (Figure 5B). This altered binding mode not only allowed a N atom in the hydrazone in **5j** to form a hydrogen bond interaction with H640 but also enabled another N atom to form new hydrogen bond interaction with E522. Moreover, the terminal benzene ring could form a new $\pi-\pi$ interaction with Y599. These new interactions may explain the stronger inhibitory activity of **5j** compared with that of **A2-4**. Figure 5C shows the differences in the binding modes of **A2-4** and **5j** in the *E. coli* PDHc-E1 active site. At the active site, **A2-4** binds in a V conformation with the terminal benzene ring near the $Mg^{2+}$ site because of the more flexible bonds in its structure. The hydrazone structural unit in **5j** increases the rigidity of the molecule and the entire molecule binds to one side of the active site in a straight conformation, which allows a new $\pi-\pi$ interaction with Y599. This new binding mode can enhance the interactions between the compound and the amino acid residues in the active site, thereby enhancing its inhibitory activity against *E. coli* PDHc-E1.

The crystal structure of porcine PDHc-E1 has not been reported. Because porcine PDHc-E1 and human PDHc-E1 have a high sequence similarity of 98.5%,[26] porcine PDHc-E1 can be considered as a representative mammal PDHc-E1. Moreover, porcine PDHc-E1 is more readily available for enzyme bioassays. Therefore, to understand the theoretical basis of the high selectivity of compounds in the **5** series, the 3D structure of porcine PDHc-E1 was first established using homology modeling with the human PDHc-E1 crystal structure (PDB ID: 3EXE)[49] as a template. The plausibility of the structure was checked using Procheck. The results indicated that more than 99% of the residue conformations fell in the plausible region (see the Ramachandran plot in the Supporting Information), which confirmed that the homology modeling was reasonable. The representative compound **5j** was docked into the active sites of *E. coli* PDHc-E1 and porcine PDHc-E1 (Figure 6). As shown in Figure 6B, the aminopyrimidine ring of **5j** could form hydrogen bonds with G136, V138, E420, and a $\pi-\pi$ interaction with F446 in the porcine PDHc-E1 active site, and only one N atom in the hydrazone structure formed a weak hydrogen bond with H489. Two new interactions were detected in the binding of **5j** to *E. coli* PDHc-E1: another N atom in the hydrazone structure formed a hydrogen bond with E522; and the terminal benzene ring formed a $\pi-\pi$ interaction with Y599 (Figure 6A). These two interactions were not detected in the binding of **5j** with porcine PDHc-E1. These differences may explain the stronger inhibitory activity of **5j** against *E. coli* PDHc-E1 than against

porcine PDHc-E1. These results shed light on the selectivity of compounds in the **5** series and lay the foundation for the design of highly selective fungicides targeting PDHc-E1 in pathogenic fungi.

To further confirm the predicted interactions of compound **5j** with *E. coli* PDHc-E1, site-directed mutagenesis and enzymatic analyses were conducted (Figure 7). The $IC_{50}$ values of **5j** against the mutants V192A (8.63 $\mu$M), M194A (6.17 $\mu$M), E571A (7.87 $\mu$M), F602A (12.65 $\mu$M), and H640A (5.43 $\mu$M) were much higher than the $IC_{50}$ against the wild-type PDHc-E1 (0.94 $\mu$M). The results confirmed that the residues V192, M194, E571, F602, and H640 play an important role in the binding of **5j** with *E. coli* PDHc-E1, as with the binding of **A2-4**. Unlike **A2-4**, **5j** also bound strongly to the residues Y599 and E522 in the active site of *E. coli* PDHc-E1. The $IC_{50}$ values of **5j** against the mutants Y599A (2.33 $\mu$M) and E522A (12.27 $\mu$M) were about 2.5-fold and 13.1-fold higher than that against the wild-type PDHc-E1, indicating that Y599 and E522 also play important roles in the binding of **5j** with *E. coli* PDHc-E1. These two new interactions resulted in the stronger inhibitory activity of **5j** than that of **A2-4** against *E. coli* PDHc-E1. Thus, the predictions based on molecular docking were consistent with the experimental results of site-directed mutagenesis.

**3.6. Antifungal Activity of Compounds.** *3.6.1. In Vitro Antifungal Activity.* The potential commercial value of compounds in the **5** series as antifungal agents was investigated by preliminary *in vitro* screening against six phytopathogenic fungi. As shown in Table 4, some compounds exhibited more than 80% inhibition of the tested fungi at 50 $\mu$g/mL. All of the **5** series compounds except **5a**, **5c**, **5d**, and **5n** showed potent antifungal activity against *M. fructigena*.

The $EC_{50}$ values of the compounds showing strong antifungal activity in the preliminary tests were further determined and compared with those of captan and chlorothalonil as positive controls. As shown in Table 5, the lead compound **A2-4** inhibited *B. cinerea* ($EC_{50}$ = 11.80 $\mu$M),[24] but its antifungal activity was weaker than those of **5f** ($EC_{50}$ = 6.53 $\mu$M), **5j** ($EC_{50}$ = 4.33 $\mu$M), **5n** ($EC_{50}$ = 4.70 $\mu$M), **5o** ($EC_{50}$ = 8.30 $\mu$M), and chlorothalonil ($EC_{50}$ = 3.57 $\mu$M), and it had very poor inhibitory activity against the other tested phytopathogenic fungi ($EC_{50}$ > 100 $\mu$M). The inhibitory activity of **5c** against *B. dothidea* ($EC_{50}$ = 3.72 $\mu$M) was 18.9-fold higher than that of captan ($EC_{50}$ = 70.50 $\mu$M) and comparable to that of chlorothalonil ($EC_{50}$ = 4.06 $\mu$M). The inhibitory activities of **5j** ($EC_{50}$ = 4.33 $\mu$M) and **5n** ($EC_{50}$ = 4.70 $\mu$M) against *B. cinerea* were 27.2-fold and 25.0-fold higher than that of captan ($EC_{50}$ = 117.60 $\mu$M), respectively. Compounds **5c** ($EC_{50}$ = 32.80 $\mu$M), **5n** ($EC_{50}$ = 11.90 $\mu$M), and **5o** ($EC_{50}$ = 16.97 $\mu$M) exhibited significant antifungal activity against *C. gloeosporioides*. In particular, the inhibitory activity of **5n** ($EC_{50}$ = 11.90 $\mu$M) was 12.6-fold higher than that of captan ($EC_{50}$ = 150 $\mu$M) and 4.4-fold higher than that of chlorothalonil ($EC_{50}$ = 52.40 $\mu$M). Most compounds in the **5** series displayed excellent antifungal activity against *M. fructigena*. Notably, the inhibitory activity of **5f** ($EC_{50}$ = 0.25 $\mu$M) was 380-fold and 8.4-fold higher than that of captan ($EC_{50}$ = 95 $\mu$M) and chlorothalonil ($EC_{50}$ = 2.11 $\mu$M), respectively. Compound **5i** was 82.6-times and 1.8-times more potent than captan ($EC_{50}$ = 1.15 $\mu$M vs 95 $\mu$M) and chlorothalonil ($EC_{50}$ = 1.15 $\mu$M vs 2.11 $\mu$M), respectively. The inhibitory activities of **5f** and **5i** against *M. fructigena* were considerably stronger than that of **A2-4** ($EC_{50}$ > 100 $\mu$M).

These results warrant further investigation of **5f** and **5i** as specific fungicides against *M. fructigena*.

Further comparison of the enzyme inhibitory and fungicidal activities of these compounds (Tables 1 and 5) revealed several interesting results: (a) The lead compound **A2-4** ($IC_{50}$ = 11.86 ± 1.01 $\mu$M), which functions as a PDHc-E1 inhibitor and binds in the *E. coli* PDHc-E1 active site in a V conformation, showed a narrow fungicidal spectrum and had limited antifungal activity against *B. cinerea* ($EC_{50}$ = 11.80 $\mu$M). However, compounds in the **5** series displayed a different binding mode from that of **A2-4**. Compounds **5** bound in a straight pattern at the active site of *E. coli* PDHc-E1 and inhibited PDHc-E1 in a competitive manner. Compared with **A2-4**, compounds **5** more strongly inhibited both *E. coli* PDHc-E1 and phytopathogenic fungi. The inhibitory activity of **5f** against *E. coli* PDHc-E1 ($EC_{50}$ = 1.03 $\mu$M) was 11.5-fold higher than that of **A2-4**. Compared with **A2-4**, **5f** showed stronger antifungal activity against *B. cinerea* ($EC_{50}$ = 6.53 $\mu$M) and showed a wider spectrum of antifungal activity. It also exhibited excellent fungicidal activity against *B. dothidea* ($EC_{50}$ = 12.24 $\mu$M), *M. poae* ($EC_{50}$ = 63.34 $\mu$M), and *M. fructigena* ($EC_{50}$ = 0.25 $\mu$M). (b) Compounds **5f** ($IC_{50}$ = 1.03 ± 0.15 $\mu$M) and **5i** ($IC_{50}$ = 1.46 ± 0.23 $\mu$M) were also potent *E. coli* PDHc-E1 inhibitors, and strongly inhibited *M. fructigena* ($EC_{50}$ = 0.25 and 1.15 $\mu$M, respectively). Both of them showed stronger inhibitory activity than that of **A2-4** ($EC_{50}$ > 100 $\mu$M), captan ($EC_{50}$ = 95 $\mu$M), and chlorothalonil ($EC_{50}$ = 2.11 $\mu$M). These results indicate that the inhibitory activity of the **5** series of compounds against *E. coli* PDHc-E1 is associated with their fungicidal activity. (c) Captan was found to be a weak PDHc-E1 inhibitor and also showed weak inhibitory activity against the five tested phytopathogenic fungi. Accordingly, the compounds in the **5** series, especially the potent PDHc-E1 inhibitor **5f**, showed superior fungicidal activity.

*3.6.2. In Vivo Antifungal Activity against M. fructigena.* Considering the excellent *in vitro* inhibitory activities of **5i** and **5f** against *M. fructigena*, their inhibition of *M. fructigena* was further tested *in vivo*. Tebuconazole, a fungicide commonly used to control brown rot fungus, was chosen as a positive control. As shown in Table 6 and Figure 8, the efficacy of compounds **5f** and **5i** against *M. fructigena* at 2.5, 5, and 10 $\mu$g/mL on day 4 ranged from 72 to 91%, which was not significantly different ($P$ < 0.05) from the efficacy of the commercial fungicide tebuconazole (78−95%). This result demonstrated that **5f** and **5i** were comparable to tebuconazole in terms of their ability to control peach brown rot caused by *M. fructigena*.

These results showed that the lead compound **A2** was optimized by modifying the linker portion and aminopyrimidine ring increased rigidity of the molecule, resulting in stronger binding of compounds in the **5** series to the active site of *E. coli* PDHc-E1. Therefore, compounds **5** as a kind of PDHc-E1 inhibitors with this novel binding mode not only displayed excellent selectivity between microbial and mammalian PDHc-E1 but also have considerably stronger antifungal activity than that of **A2**, captan, and chlorothalonil. In particular, **5f** and **5i** have the potential for application as fungicides against *M. fructigena*. To the best of our knowledge, these compounds are the most active antifungal agents as PDHc-E1 inhibitors identified to date.

## AUTHOR INFORMATION

**Corresponding Author**

**Hongwu He** − *Key Laboratory of Pesticide and Chemical Biology of Ministry of Education, College of Chemistry, Central China Normal University, Wuhan 430079, P. R. China;* orcid.org/0000-0003-1470-2794; Phone: +86 (0)27 67867960; Email: he1208@mail.ccnu.edu.cn

**Authors**

**Yuan Zhou** − *Key Laboratory of Pesticide and Chemical Biology of Ministry of Education, College of Chemistry, Central China Normal University, Wuhan 430079, P. R. China;* orcid.org/0000-0002-4743-467X

**Shasha Zhang** − *Key Laboratory of Pesticide and Chemical Biology of Ministry of Education, College of Chemistry, Central China Normal University, Wuhan 430079, P. R. China*

**Meng Cai** − *Key Laboratory of Pesticide and Chemical Biology of Ministry of Education, College of Chemistry, Central China Normal University, Wuhan 430079, P. R. China*

**Kaixing Wang** − *Key Laboratory of Pesticide and Chemical Biology of Ministry of Education, College of Chemistry, Central China Normal University, Wuhan 430079, P. R. China*

**Jiangtao Feng** − *Key Laboratory of Pesticide and Chemical Biology of Ministry of Education, College of Chemistry, Central China Normal University, Wuhan 430079, P. R. China*

**Dan Xie** − *Key Laboratory of Pesticide and Chemical Biology of Ministry of Education, College of Chemistry, Central China Normal University, Wuhan 430079, P. R. China*

**Lingling Feng** − *Key Laboratory of Pesticide and Chemical Biology of Ministry of Education, College of Chemistry, Central China Normal University, Wuhan 430079, P. R. China;* orcid.org/0000-0003-1260-4656

**Hao Peng** − *Key Laboratory of Pesticide and Chemical Biology of Ministry of Education, College of Chemistry, Central China Normal University, Wuhan 430079, P. R. China*

Complete contact information is available at:
https://pubs.acs.org/10.1021/acs.jafc.0c07701

**Author Contributions**

[†]Y.Z. and S.Z. equally contributed to this work.

**Notes**

The authors declare no competing financial interest.

## ■ REFERENCES

(1) Yin, X. D.; Ma, K. Y.; Wang, Y. L.; Sun, Y.; Shang, X. F.; Zhao, Z. M.; Wang, R. X.; Chen, Y. J.; Zhu, J. K.; Liu, Y. Q. Design, synthesis, and antifungal evaluation of 8-hydroxyquinoline metal complexes against phytopathogenic fungi. *J. Agric. Food Chem.* **2020**, *68*, 11096−11104.

(2) Wu, Y. Y.; Shao, W. B.; Zhu, J. J.; Long, Z. Q.; Liu, L. W.; Wang, P. Y.; Li, Z.; Yang, S. Novel 1,3,4-oxadiazole-2-carbohydrazides as prospective agricultural antifungal agents potentially targeting succinate dehydrogenase. *J. Agric. Food Chem.* **2019**, *67*, 13892−13903.

(3) Yang, G. Z.; Zhu, J. K.; Yin, X. D.; Yan, Y. F.; Wang, Y. L.; Shang, X. F.; Liu, Y. Q.; Zhao, Z. M.; Peng, J. W.; Liu, H. Design, synthesis, and antifungal evaluation of novel quinoline derivatives inspired from natural quinine alkaloids. *J. Agric. Food Chem.* **2019**, *67*, 11340−11353.

(4) Wang, L. L.; Li, C.; Zhang, Y. Y.; Qiao, C. H.; Ye, Y. H. Synthesis and biological evaluation of benzofuroxan derivatives as fungicides against phytopathogenic fungi. *J. Agric. Food Chem.* **2013**, *61*, 8632−8640.

(5) Obydennov, K. L.; Khamidullina, L. A.; Galushchinskiy, A. N.; Shatunova, S. A.; Kosterina, M. F.; Kalinina, T. A.; Fan, Z. J.; Glukhareva, T. V.; Morzherin, Y. Y. Discovery of methyl (5Z)-[2-(2,4,5-trioxopyrrolidin-3-ylidene)-4-oxo-1,3-thiazolidin-5-ylidene]-acetates as antifungal agents against potato diseases. *J. Agric. Food Chem.* **2018**, *66*, 6239−6245.

(6) Liu, Y. X.; Song, H. J.; Huang, Y. Q.; Li, J. R.; Zhao, S.; Song, Y. C.; Yang, P. W.; Xiao, Z. X.; Liu, Y. X.; Li, Y. Q.; Shang, H.; Wang, Q. M. Design, synthesis, and antiviral, fungicidal, and insecticidal activities of tetrahydro-β-carboline-3-carbohydrazide derivatives. *J. Agric. Food Chem.* **2014**, *62*, 9987−9999.

(7) Patel, M. S.; Korotchkina, L. G. The biochemistry of the pyruvate dehydrogenase complex. *Biochem. Mol. Biol. Educ.* **2003**, *31*, 5−15.

(8) Nemeria, N.; Baykal, A.; Joseph, E.; Zhang, S.; Yan, Y.; Furey, W.; Jordan, F. Tetrahedral intermediates in thiamin diphosphate-dependent decarboxylations exist as a 1′,4′-imino tautomeric form of the coenzyme, unlike the michaelis complex or the free coenzyme. *Biochemistry* **2004**, *43*, 6565−6575.

(9) Dugger, W. M.; Humphreys, T. E.; Calhoun, B. Influence of N-(trichloromethylthio)-4-cyclohexene-1,2-dicarboximide (Captan) on higher plants. II. Effect on specific enzyme systems. *Am. J. Bot.* **1959**, *46*, 151−156.

(10) Balakrishnan, A.; Nemeria, N. S.; Chakraborty, S.; Kakalis, L.; Jordan, F. Determination of pre-steady-state rate constants on the *Escherichia coli* pyruvate dehydrogenase complex reveals that loop movement controls the rate-limiting step. *J. Am. Chem. Soc.* **2012**, *134*, 18644−18655.

(11) Schellenberger, A. Die funktion der 4′-aminopyrimidin-komponente im katalysemechanismus von thiaminpyrophosphat-enzymen aus heutiger sicht. *Chem. Ber.* **1990**, *123*, 1489−1494.

(12) Wittorf, J. H.; Gubler, C. J. Coenzyme binding in yeast pyruvate decarboxylase. *Eur. J. Biochem.* **1971**, *22*, 544−550.

(13) Shreve, D. S.; Holloway, M. P.; Haggerty, J. C.; Sable, H. Z. The catalytic mechanism of transketolase. Thiamin pyrophosphate-derived transition states for transketolase and pyruvate dehydrogenase are not identical. *J. Biol. Chem.* **1983**, *258*, 12405−12408.

(14) Kluger, R.; Gish, G.; Kauffman, G. Interaction of thiamin diphosphate and thiamin thiazolone diphosphate with wheat germ pyruvate decarboxylase. *J. Biol. Chem.* **1984**, *259*, 8960−8965.

(15) Tripatara, A.; Korotchkina, L. G.; Patel, M. S. Characterization of point mutations in patients with pyruvate dehydrogenase deficiency: role of methionine-181, proline-188, and arginine-349 in the α subunit. *Arch. Biochem. Biophys.* **1999**, *367*, 39−50.

(16) Lowe, P. N.; Leeper, F. J.; Perham, R. N. Stereoisomers of tetrahydrothiamin pyrophosphate, potent inhibitors of the pyruvate dehydrogenase multienzyme complex from *Escherichia coli*. *Biochemistry* **1983**, *22*, 150−157.

(17) Hawksley, D.; Griffin, D. A.; Leeper, F. J. Synthesis of 3-deazathiamine. *J. Chem. Soc., Perkin Trans. 1* **2001**, *2*, 144−148.

(18) Leeper, F. J.; Hawksley, D.; Mann, S.; Melero, C. P.; Wood, M. D. H. Studies on thiamine diphosphate-dependent enzymes. *Biochem. Soc. Trans.* **2005**, *33*, 772−775.

(19) Mann, S.; Melero, C. P.; Hawksley, D.; Leeper, F. J. Inhibition of thiamin diphosphate dependent enzymes by 3-deazathiamin diphosphate. *Org. Biomol. Chem.* **2004**, *2*, 1732−1741.

(20) Erixon, K. M.; Dabalos, C. L.; Leeper, F. J. Synthesis and biological evaluation of pyrophosphate mimics of thiamine pyrophosphate based on a triazole scaffold. *Org. Biomol. Chem.* **2008**, *6*, 3561−3572.

(21) Erixon, K. M.; Dabalos, C. L.; Leeper, F. J. Inhibition of pyruvate decarboxylase from *Z. mobilis* by novel analogues of thiamine pyrophosphate: investigating pyrophosphate mimics. *Chem. Commun.* **2007**, *9*, 960−962.

(22) Arjunan, P.; Nemeria, N.; Brunskill, A.; Chandrasekhar, K.; Sax, M.; Yan, Y.; Jordan, F.; Guest, J. R.; Furey, W. Structure of the pyruvate dehydrogenase multienzyme complex E1 component from *Escherichia coli* at 1.85 Å resolution. *Biochemistry* **2002**, *41*, 5213−5221.

(23) He, J. B.; Feng, L. L.; Li, J.; Tao, R. J.; Wang, F.; Liao, X.; Sun, Q. S.; Long, Q. W.; Ren, Y. L.; Wan, J.; He, H. W. Design, synthesis and biological evaluation of novel 2-methylpyrimidine-4-ylamine derivatives as inhibitors of *Escherichia coli* pyruvate dehydrogenase complex E1. *Bioorg. Med. Chem.* **2012**, *20*, 1665−1670.

(24) He, J. B.; He, H. F.; Zhao, L. L.; Zhang, L.; You, G. Y.; Feng, L. L.; Wan, J.; He, H. W. Synthesis and antifungal activity of 5-iodo-1,4-disubstituted-1,2,3-triazole derivatives as pyruvate dehydrogenase complex E1 inhibitors. *Bioorg. Med. Chem.* **2015**, *23*, 1395−1401.

(25) He, J. B.; Ren, Y. L.; Sun, Q. S.; You, G. Y.; Zhang, L.; Zou, P.; Feng, L. L.; Wan, J.; He, H. W. Design, synthesis and molecular docking of amide and urea derivatives as *Escherichia coli* PDHc-E1 inhibitors. *Bioorg. Med. Chem.* **2014**, *22*, 3180−3186.

(26) Zhou, Y.; Zhang, S. S.; He, H. W.; Jiang, W.; Hou, L. F.; Xie, D.; Cai, M.; Peng, H.; Feng, L. L. Design and synthesis of highly selective pyruvate dehydrogenase complex E1 inhibitors as bactericides. *Bioorg. Med. Chem.* **2018**, *26*, 84−95.

(27) Feng, L. L.; He, J. B.; He, H. F.; Zhao, L. L.; Deng, L. F.; Zhang, L.; Zhang, L.; Ren, Y. L.; Wan, J.; He, H. W. The design, synthesis and biological evaluation of novel thiamin diphosphate analog inhibitors against the pyruvate dehydrogenase multienzyme complex E1 from *Escherichia coli*. *Org. Biomol. Chem.* **2014**, *12*, 8911−8918.

(28) He, J. B.; Feng, L. L.; Li, J.; Tao, R. J.; Ren, Y. L.; Wan, J.; He, H. W. Design, synthesis and molecular modeling of novel N-acylhydrazone derivatives as pyruvate dehydrogenase complex E1 inhibitors. *Bioorg. Med. Chem.* **2014**, *22*, 89−94.

(29) Zhou, Y.; Feng, J. T.; Feng, L. L.; Xie, D.; Peng, H.; Cai, M.; He, H. W. Synthesis and activity of 1,2,3-triazole aminopyrimidines against cyanobacteria as PDHc-E1 competitive inhibitors. *J. Agric. Food Chem.* **2019**, *67*, 12538−12546.

(30) He, H. F.; Feng, J. T.; He, J. B.; Xia, Q.; Ren, Y. L.; Wang, F.; Peng, H.; He, H. W.; Feng, L. L. Design, synthesis, biological evaluation and molecular docking of amide and sulfamide derivatives as *Escherichia coli* pyruvate dehydrogenase complex E1 inhibitors. *RSC Adv.* **2016**, *6*, 4310−4320.

(31) Feng, J. T.; He, H. F.; Zhou, Y.; Guo, X. L.; Liu, H. L.; Cai, M.; Wang, F.; Feng, L. L.; He, H. W. Design, synthesis and biological evaluation of novel inhibitors against cyanobacterial pyruvate dehydrogenase multienzyme complex E1. *Bioorg. Med. Chem.* **2019**, *27*, 2413−2420.

(32) Feng, J. T.; He, H. F.; Zhou, Y.; Cai, M.; Peng, H.; Liu, H. L.; Liu, L.; Feng, L. L.; He, H. W. Structure optimization and bioactivity evaluation of ThDP analogs targeting cyanobacterial pyruvate dehydrogenase E1. *Bioorg. Med. Chem.* **2019**, *27*, No. 115119.

(33) He, H. F.; Wang, W.; Zhou, Y.; Xia, Q.; Ren, Y. L.; Feng, J. T.; Peng, H.; He, H. W.; Feng, L. L. Rational design, synthesis and biological evaluation of 1,3,4-oxadiazole pyrimidine derivatives as novel pyruvate dehydrogenase complex E1 inhibitors. *Bioorg. Med. Chem.* **2016**, *24*, 1879−1888.

(34) Zhou, Y.; Feng, J. T.; He, H. W.; Hou, L. F.; Jiang, W.; Xie, D.; Feng, L. L.; Cai, M.; Peng, H. Design, synthesis, and potency of pyruvate dehydrogenase complex E1 inhibitors against cyanobacteria. *Biochemistry* **2017**, *56*, 6491−6502.

(35) Pei, X. Y.; Titman, C. M.; Frank, R. A. W.; Leeper, F. J.; Luisi, B. F. Snapshots of catalysis in the E1 subunit of the pyruvate dehydrogenase multienzyme complex. *Structure* **2008**, *16*, 1860−1872.

(36) Arjunan, P.; Chandrasekhar, K.; Sax, M.; Brunskill, A.; Nemeria, N.; Jordan, F.; Furey, W. Structural determinants of enzyme binding affinity: the E1 component of pyruvate dehydrogenase from *Escherichia coli* in complex with the inhibitor thiamin thiazolone diphosphate. *Biochemistry* **2004**, *43*, 2405−2411.

(37) Pei, X. Y.; Erixon, K. M.; Luisi, B. F.; Leeper, F. J. Structural insights into the prereaction state of pyruvate decarboxylase from *Zymomonas mobilis*. *Biochemistry* **2010**, *49*, 1727−1736.

(38) Zhang, M.; Dai, Z. C.; Qian, S. S.; Liu, J. Y.; Xiao, Y.; Lu, A. M.; Zhu, H. L.; Wang, J. X.; Ye, Y. H. Design, synthesis, antifungal, and antioxidant activities of (E)-6-((2-phenylhydrazono)methyl)-quinoxaline derivatives. *J. Agric. Food Chem.* **2014**, *62*, 9637−9643.

(39) Kodisundaram, P.; Amirthaganesan, S.; Balasankar, T. Antimicrobial evaluation of a set of heterobicyclic methylthiadiazole hydrazones: synthesis, characterization, and SAR studies. *J. Agric. Food Chem.* **2013**, *61*, 11952−11956.

(40) Watt, M.; Hardebeck, L. K. E.; Kirkpatrick, C. C.; Lewis, M. Face-to-face arene-arene binding energies: dominated by dispersion but predicted by electrostatic and dispersion/polarizability substituent constants. *J. Am. Chem. Soc.* **2011**, *133*, 3854−3862.

(41) Ferlin, M. G.; Di Marco, V. B.; Dean, A. Synthesis of 1,4-dihydro-2-methyl-4-oxo-nicotinic acid: Ochiai's route failed. *Tetrahedron* **2006**, *62*, 6222−6227.

(42) Wang, X.; Chen, Y. F.; Yan, W.; Cao, L. L.; Ye, Y. H. Synthesis and biological evaluation of benzimidazole phenylhydrazone derivatives as antifungal agents against phytopathogenic fungi. *Molecules* **2016**, *21*, No. 1574.

(43) Ren, Y. L.; He, J. B.; Feng, L. L.; Liao, X.; Jin, J.; Li, Y. J.; Cao, Y.; Wan, J.; He, H. W. Structure-based rational design of novel hit compounds for pyruvate dehydrogenase multienzyme complex E1 components from *Escherichia coli*. *Bioorg. Med. Chem.* **2011**, *19*, 7501−7506.

(44) Feng, L. L.; Sun, Y.; Deng, H.; Li, D.; Wan, J.; Wang, X. F.; Wang, W. W.; Liao, X.; Ren, Y. L.; Xu, X. P. Structural and biochemical characterization of fructose-1,6/sedoheptulose-1,7-bisphosphatase from the cyanobacterium Synechocystis strain 6803. *FEBS J.* **2014**, *281*, 916−926.

(45) Waterhouse, A.; Bertoni, M.; Bienert, S.; Studer, G.; Tauriello, G.; Gumienny, R.; Heer, F. T.; de Beer, T. A. P.; Rempfer, C.; Bordoli, L.; Lepore, R.; Schwede, T. Swiss-model: homology modelling of protein structures and complexes. *Nucleic Acids Res.* **2018**, *46*, W296−W303.

(46) Cai, M.; Miao, J. Q.; Song, X.; Lin, D.; Bi, Y.; Chen, L.; Liu, X. L.; Tyler, B. M. C239S mutation in the *β*-tubulin of phytophthora sojae confers resistance to Zoxamide. *Front. Microbiol.* **2016**, *7*, No. 762.

(47) Chen, F. P.; Fan, J. R.; Zhou, T.; Liu, X. L.; Liu, J. L.; Schnabel, G. Baseline sensitivity of *Monilinia fructicola* from China to the DMI fungicide SYP-Z048 and analysis of DMI-Resistant Mutants. *Plant Dis.* **2012**, *96*, 416−422.

(48) He, H. F.; Xia, Q.; He, H. W. Synthesis and biological evaluation of pyrimidine derivatives containing hydrazine structural unit. *Chin. J. Org. Chem.* **2019**, *39*, 2295−2302.

(49) Kato, M.; Wynn, R. M.; Chuang, J. L.; Tso, S. C.; Machius, M.; Li, J.; Chuang, D. T. Structural basis for inactivation of the human pyruvate dehydrogenase complex by phosphorylation: role of disordered phosphorylation loops. *Structure* **2008**, *16*, 1849−1859.